Catalysis Today xxx (xxxx) xxx

Contents lists available at ScienceDirect

Catalysis Today

journal homepage: www.elsevier.com/locate/cattod

Classical and new insights into the methodology for characterizing adsorbents and metal catalysts by chemical adsorption

A. Gil

INAMAT˜2-Departamento de Ciencias, Edificio de los Acebos, Universidad Pública de Navarra, Campus de Arrosadía, E-31006 Pamplona, Spain

ARTICLE INFO

Keywords:
Chemical adsorption
Selective adsorption
Active sites
Metallic dispersion
Metallic surface area
Acid/base properties

ABSTRACT

The adsorption phenomenon has been used extensively to achieve and explain solid-state reactions, control contamination, and purify liquids and gases. This process implies the use of a porous medium or a material with specific adsorption centers where the interactions with the reagents occur. Determination of the properties of adsorbent or catalyst materials that do not contain specific adsorption sites by physical gas adsorption is a well-established procedure in most research and quality-control laboratories. However, characterizing the specific centers by selective adsorption—chemisorption—remains an open question for discussion and study. The specific centers involved are often acidic/basic and metallic; in most cases, reagents are adsorbed and desorbed in these centers, whose determination allows controlling the processes and comparing the materials. The techniques and procedures presented herein facilitate the evaluation and the qualitative and quantitative determination of the surface properties of the materials using chemisorption processes for metallic and acidic/basic sites. The aim of this work is to review these techniques and procedures, including the updates published by several researchers, who mostly strive to explain the results of bifunctional metallic and acid–base catalytic behavior.

1. Introduction

In order to understand the processes occurring on the surface of adsorbents and catalysts and thus be able to modify and optimize them, we need to study their surface properties. In the case of supported metal catalysts, the metal surface must be exposed to these processes, in other words the metal must be dispersed in order to be accessible. This process can be performed during the early stages of the material preparation method [1,2]. Therefore, being able to analyze and characterize a metal that is dispersed in small particles on a surface is of vital importance. In general, the surface structure of a metallic crystal varies greatly depending on the size of the particles and, especially, on how they are found on the surface of a support and their size distribution. Likewise, the surface of the support may affect the properties of the particles, making them different to those of isolated particles. Similarly, the acid–base properties of catalytic supports and catalysts are also important as they may affect catalyst preparation [1,2], and play a role in the mechanism of the reactions [1]. In order to understand the catalytic and adsorption behavior, evaluating the properties of such materials is essential.

The dispersion of a supported metal is defined as the fraction of metal atoms found on its surface and can be related to the number of metal centers accessible to reactants and products [1]. Understanding this dispersion is crucial to interpret the kinetic data of a catalytic reaction and to compare catalysts of the same family; the Turn Over Frequency (TOF), defined as the number of molecules reacting per active site per second or the number of molecules reacting per surface metal atom per second, is key for this purpose. As such, several techniques have been proposed and used to measure the TOF, including transmission electron microscopy and X-ray diffraction; the most widely used, however, is surface and selective gas adsorption [2–5]. Chemisorption methods are particularly important for highly dispersed catalysts given the difficulty in estimating their dispersion using other techniques, such as X-ray diffraction or electron microscopy. The most frequently used gases in chemisorption are H_2, CO, O_2 and even N_2O. Other gases are used in specific cases, such as NO, H_2S, CS_2, C_6H_6, etc. Several organizations (e.g., American Society for Testing and Materials - ASTM; International Union of Pure and Applied Chemistry-IUPAC) have provided guidance for analyzing the surface of metals, generally recommending hydrogen as an adsorbent [6]. Hydrogen has the advantage of being mainly chemisorbed on the metallic part of the surface, and the amount retained on the non-metallic part is relatively small and weak in many cases. Hydrogen is physically adsorbed on metallic and non-metallic parts, but when measuring at room temperature and pressure, the contribution of

E-mail address: andoni@unavarra.es.

https://doi.org/10.1016/j.cattod.2023.01.023
Received 12 December 2022; Received in revised form 15 January 2023; Accepted 24 January 2023
Available online 25 January 2023

the physically adsorbed layer can be neglected due to the very small adsorption enthalpy of hydrogen (less than 8 kJ/mol). However, an exception may be necessary for activated carbon and MOFs as supports, especially when this material has a high specific surface area. Indeed, these materials, which can have a surface area of 5000 m^2/g and sometimes more, have been used in H_2 storage [7]. These values can be corrected by measuring the physical adsorption of hydrogen on the metal-free support separately. CO adsorption also allows the determination of metallic surfaces, since there is a specific reaction between the gas molecule and the metal. The main drawback of CO chemisorption is determining the CO/metal stoichiometry, since the CO molecule can form various types of bonds with the metal, as well as polynuclear complexes [8]. Transmission electron microscopy, in turn, has the great advantage of providing a direct view of the particles to be analyzed. This analysis allows the size distribution and all its characteristic parameters to be obtained, and shows whether the particles formed are large, what shape they have, and it is even possible to determine their crystal structure. In the case of X-ray diffraction, measurement of the size of metal crystallites is based on the presence of diffraction lines provided the particles are sufficiently small. Quantitatively, it can be determined using the Scherrer equation, which relates the average diameter of the crystals to the broadening of the diffraction peaks. The disadvantage of this technique is that it can only be applied to samples presenting a diffraction line, which means that it cannot be used for catalysts with a very low metal loading (less than 1 % by weight, although this value depends on the metal). Crystalline supports or supports presenting diffraction lines can interfere with the determination of the diffraction lines. In general, glass particles with a size of between 5 and 50 nm can be determined. In conclusion, most authors/researchers indicate that selective gas chemisorption is the best method for characterizing/determining the active surface of a metal catalyst, due to several reasons, especially to its easy accessibility, however, other techniques may be necessary to corroborate the presence of very large crystal materials.

Acid catalysts are very important in alkylation, dealkylation, cracking, hydrocracking, isomerization and reforming reactions [1], all of which are used in petroleum refinery processes. Two types of acid centers can be distinguished: Lewis and Brönsted. Lewis centers accept a pair of electrons from the adsorbed species to form a coordination bond between the adsorbed molecule and the solid surface. Brönsted centers however, provide a proton to the adsorbed molecule to form an ion-dipole interaction between the adsorbed species and the solid surface. Both types of centers are found in alumina, for example [1], where aluminum acts as the Lewis acid center and the OH groups on the surface as the Brönsted centers. Characterization of surface acidity is normally performed using techniques such as infrared spectroscopy, NMR spectroscopy, thermal analysis and titration with basic molecules such as ammonia or pyridine (C_5H_5N), although numerous studies have rather focused on temperature-programmed desorption (TPD). Base catalysis is less widespread than acid catalysis—as it provides lower yields—although it is more selective than the latter. Lewis bases act as an electron donor and can be related to the surface lattice oxygen, O^{2-}. Pyrrole (C_4H_5N), deuterated chloroform ($CDCl_3$), H_2S and CO_2 have been suggested as probe molecules [9,10]. Other applications in which the surface nature of the materials may also be important—such as the use of silicates as anticorrosive agents, preventing the deterioration of washing machines, zeolitic materials as ion exchangers, activated carbons with a hydrophilic character applied as adsorbents—are also worth mentioning.

A several of factors that can affect gas chemisorption measurements have been reported, for instance the presence of impurities in the catalysts, surface reconstruction due to sintering during adsorption, the nature of metal/support interactions, *spillover* of the H_2 molecule, and even the contamination of gases used in chemisorption [11,12]. In catalytic supports such as TiO_2, V_2O_3, CeO_2—which exhibit a high degree of reactivity with metals—supported metal particles and other metal species originating from the "strong metal–support interaction" (*SMSI*) can occur; this phenomenon reduces the adsorption capacity of the metal [13]. The *SMSI* state enables the metallic particles to present reversible characteristics, that is, reduction of the particles at low temperatures allows them to be in their metallic state, while the same process at high temperature favors the *SMSI* state. This state causes the support to develop semiconductor and even metallic properties that differ from those presented initially. Several models have been proposed to explain the *SMSI* phenomenon. One of these is the formation of metallic alloys, and another proposes that the reduced species on the support can present high mobility and are capable of coating the metallic particles, thereby blocking their adsorption capacity [13]. In the case of the *spillover* phenomenon, this involves the transport of active species adsorbed or formed in a first phase (structure) to another in which they are not generated directly under the same conditions. The most common example is hydrogen adsorbed from the gas phase onto a metal (Pt, Pd, Ni, etc.), where it dissociates into atomic hydrogen. The dissociated hydrogen can subsequently be transported to the support. This phenomenon causes more hydrogen to be adsorbed than is necessary in the chemisorption process, thereby interfering with monolayer volume determinations. Thus, concludes into erroneous dispersion results.

The techniques and procedures presented below are often routine in many laboratories, since they allow the evaluation and determination of the surface properties of materials through chemisorption processes. The aim of this work is to review them and include the updates published by several researchers, who mostly aim to explain the results of bifunctional metallic and acid–base catalytic behavior.

2. Physical and chemical adsorption

Two phenomena can be observed in the adsorption process: physisorption and chemisorption [14]. In general, differentiating between these two processes is not easy, especially since intermediate behaviors can occur. Interactions between the adsorbent surface and the adsorbate are generally relatively weak via coulombic and dispersion forces, although defection at the atomic level or atoms with the availability to form bonds may be present on the surface. In such a case, chemical bonds can be formed and the process is known as chemisorption. This process often occurs at temperatures higher than the critical temperature of the adsorbate. Chemical adsorption is often irreversible, at least under mild conditions, and is characterized by large interaction potentials that lead to high adsorption heats, although this factor is not the only aspect that differentiates physisorption from chemisorption.

Physical and chemical adsorption are usually characterized by the following properties:

In **physical adsorption**, the gas molecules interact with the solid surface via van der Waals-type forces. This type of interaction determines the characteristics of the adsorption:

- physical adsorption involves a weak interaction between gas molecules and the surface of the solid. As such, no surface modifications occur during adsorption measurements;
- physical adsorption is an exothermic process: the interaction forces are attractive, and the heat released is similar to the enthalpies of condensation of the adsorbed substance (20–40 kJ/mol). As this process is exothermic, physisorption increases with decreasing the adsorbent temperature or increasing the adsorbate pressure;
- the physisorbed molecule maintains its identity, since the energy is insufficient to break the bond, although its geometry can be distorted.
- physisorption is a non-specific process, since the forces involved are not specific either. Molecules do not usually interact with specific adsorption centers.
- physisorption occurs in multilayers, meaning that another layer can be adsorbed on top of a layer of adsorbed molecules. The first

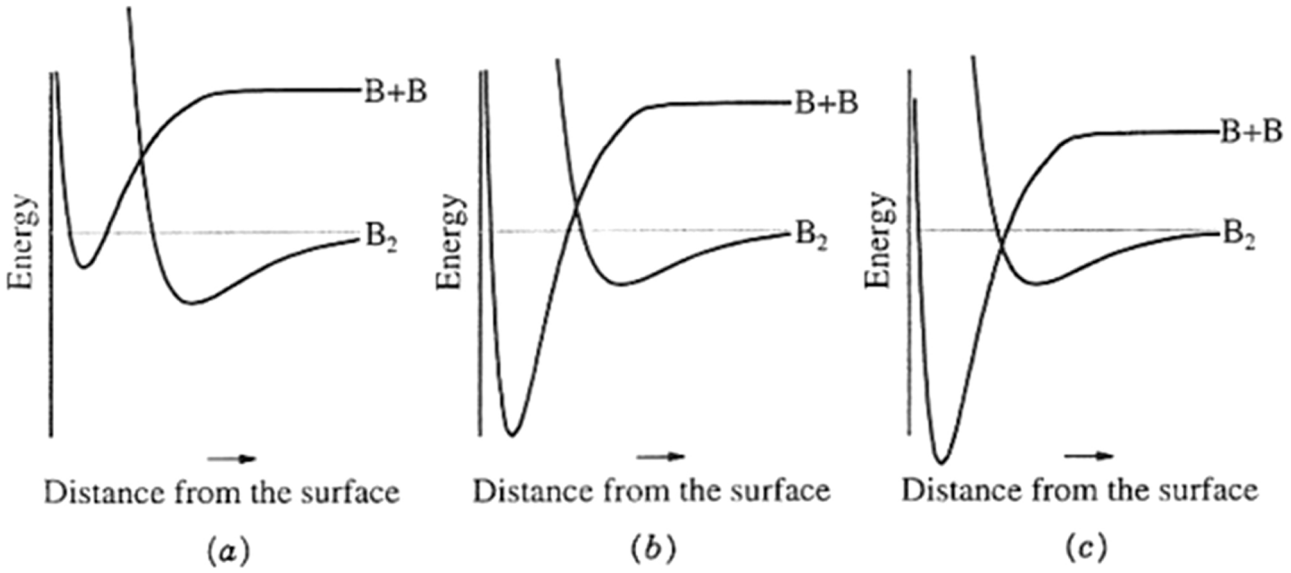

Fig. 1. One-dimensional models of the Lennard–Jones potential energy diagram corresponding to (a) molecular adsorption, (b) activated dissociative adsorption, and (c) unactivated dissociative adsorption [15].

adsorbed layer is formed by direct interaction with the surface, while the successive ones are interactions between molecules, like the condensation process. However, the difference between these two processes is not so clear and we often find intermediate situations, especially when the chemisorption process is weak.

In **chemical adsorption**, the gas molecules interact with the solid surface through chemical bonds. Similarly, to physical adsorption, this type of strong interaction conditions the characteristics of the adsorption:

- in chemical adsorption, the interaction forces are attractive, and the heats released are similar to the enthalpies of formation of a chemical bond (100–500 kJ/mol). In chemisorption, both bond formation and bond breakage can occur, so the values of these enthalpies can be both positive and negative.
- as there is a strong interaction—bond formation—between the molecule and the adsorption center, chemical adsorption is only defined in a monolayer. In the rest of the layers, physical adsorption may occur.
- if a chemical bond is formed, the chemisorbed molecule does not maintain the same structure as in the gas phase.
- chemisorption is specific. There are certain centers on the surface of the solid at which interaction occurs whereas at others it does not.

The two adsorption processes (physical and chemical) can be illustrated by representing the evolution of the potential energy of a gaseous diatomic molecule in the vicinity of a surface, where attractive and repulsive forces may appear (Fig. 1) [15]. This figure includes the option of diatomic adsorption or bond cleavage and atomic adsorption. If adsorption occurs, the potential energy decreases, thus implying that the concentration of the gas will be higher on the surface than inside the gas, due to the adsorption phenomenon. In this situation, if the gas molecule is very close to the surface of the adsorbent, the potential increases again because of the repulsion effect. The figure illustrates how molecule B_2 approaches the surface of a material at a distance *r*. The first interaction process is physical adsorption of the molecule on the surface of the solid. The equilibrium situation is represented by the potential minimum or adsorption potential well, which is characterized by a negative energy value (exothermic process). Below is an endothermic process in which an energy *E* must be overcome. If this energy value is exceeded, a new equilibrium situation can be reached but, in this situation, dissociation of the diatomic molecule occurs. Each of these situations depends on the adsorbate/adsorbent system and the temperature of the adsorption process. Three situations are represented in the figure. In the first (a), the molecule is more strongly adsorbed (its equilibrium state has a lower energy) than in the dissociated state. This the preferred form of adsorption and could represent physical adsorption. In the second case (b), the dissociated situation has a higher adsorption energy than the diatomic molecule, but there is an energy barrier to overcome. If this barrier is high enough, we would have the first case. Finally, the third case (c) is similar to the previous one, but with a very low energy barrier, so dissociated adsorption normally occurs.

The bond between the chemisorbed molecule and the adsorption center is often very energetic, even though the net heat of adsorption may be low. The requirement to overcome an activation energy in chemisorption explains the low heat of adsorption and also why such a phenomenon can be relatively slow. Since chemisorption is often an activated process, the net heat of adsorption is small at low temperatures and large at high temperatures. This situation means that physisorption predominates at low temperatures and chemisorption at higher temperatures.

3. Experimental procedure: how the amount of adsorbed gas is determined experimentally

In contrast to measurement of the specific surface area, the surface area of a catalyst component, usually the metal surface, can be measured using selective adsorption (chemisorption). The principle of selective surface area measurement by chemisorption is similar to specific surface area measurement by physisorption. As such, it will be necessary to make a series of assumptions: the metallic surface is free from other adsorbates such as carbon or other poisons that prevent or affect the gas–solid interaction; metal atoms must be in its normal metal state (normally zero) that allows interaction; and the stoichiometry of the interaction must be known and be independent of the size of the metal crystal [11,12]. As such, preparation and pretreatment of the sample have to be more rigorous than when characterization is carried out by physisorption. Intrinsic to each of the techniques to be used, the kinetics and strength of the adsorption are important aspects that must be evaluated. The techniques that allow the chemical adsorption process to be analyzed and, therefore, the active sites (acid-basic and metallic

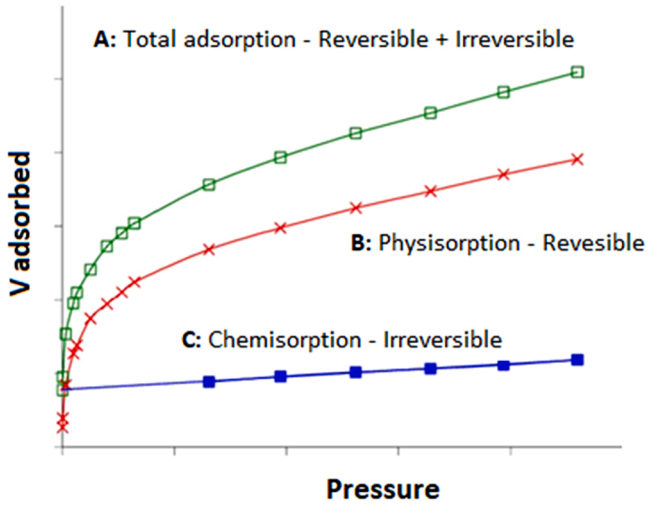

Fig. 2. Gas adsorption at constant temperature on a porous material. **A** represents the total adsorption (reversible + irreversible), **B** represents only the physisorption (reversible), adsorption repeated under the same conditions as **A**, and **C** is the difference between **A** and **B**.

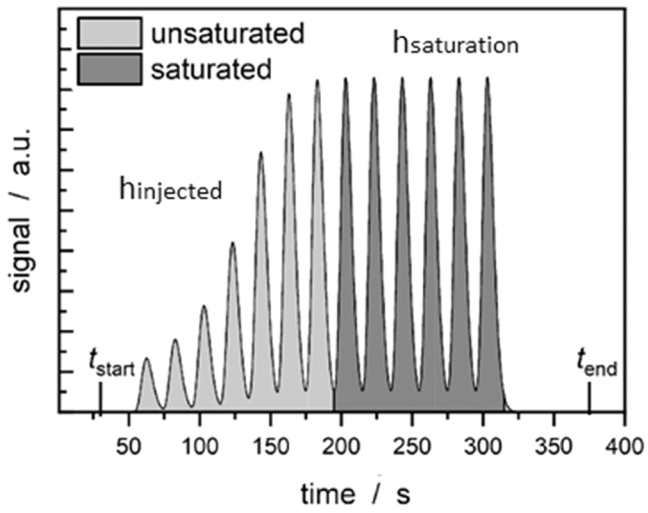

Fig. 3. Evolution of the consecutive injected pulses of an adsorbent gas on a porous solid continuously subjected to a carrier gas. The injected pulses reach saturation, at which point the solid no longer adsorbs gas [18].

adsorption centers) to be characterized, can be divided into three categories: volumetric static, gravimetric, and dynamic flow methods (isothermal or programmed temperature) [11,12].

3.1. Static volumetric procedure

Several studies have been performed by static volumetric and the unit descriptions have been published by various authors [11,12]. The materials to be characterized can present a wide distribution of active centers, either in terms of acid–base strength or metal particle sizes. These characteristics call for a technique that allows this analysis, thus meaning that the adsorbate gas must be added in small quantities in a controlled manner. Under these conditions, a technique such as the static volumetric method can guarantee low-pressure dosing of adsorbate gas, thus, could identify the different adsorption layers. The chemisorption isotherm is described as the variation in the amount of gas adsorbed as a function of pressure at equilibrium while maintaining the sample at a constant temperature. In a previous step, the surface of the sample must be cleaned with a vacuum; in many cases, pre-treatment with a cleaning gas current is preferable or even—if the chemisorption is to be conducted on a metal catalyst—reduction of the oxides so that it is in the form of a metal as this is the sensitive phase for the adsorption of gases such as H_2, CO, etc. Chemisorption isotherms are expressed in terms of amount adsorbed at normal conditions (NTP) versus absolute pressure, rather than amount adsorbed versus relative pressure, as in the case of physical adsorption. The static volumetric technique generally produces an experimental adsorption isotherm similar to that shown in Fig. 2, which involves a combination of physisorption, *spillover* and chemisorption. Hence, it is not a purely type-I isotherm with an adsorption plateau (constant amount adsorbed) as pressure increases. To differentiate the contribution of chemisorption from that of physisorption, the sample is evacuated after completion of the initial run, thus removing only reversibly adsorbed gas. The analysis is then repeated under the same conditions as the original analysis, except that during the second analysis, the active area of the sample is already saturated with chemisorbed molecules. Some authors have criticized the application of this second isotherm given that a greater amount of gas can be desorbed than the purely thermodynamic one; therefore, identical vacuum conditions to those used in the first isotherm and treatment time of up to 30 min [16]. The adsorbed volume data for the first adsorption isotherm A are a combination of physical and chemical adsorption (reversible and irreversible, respectively). Isotherm B is the result of repeated analysis, where only reversible physisorption occurs. The isotherm represented by the dashed line C is generated mathematically by subtracting the adsorbed volume data for isotherm B from that for isotherm A. The result is the amount of active gas irreversibly absorbed by the sample.

As in physisorption, the adsorption isotherm allows qualitative characterization of the material. For quantitative characterization, the volume of the monolayer (V_m) chemisorbed on an active surface is determined. One way to determine this volume is by extending a line tangential to the plateau of the initial adsorption isotherm to the zero pressure axis. This is the procedure proposed in the ASTM D 3908–88 method to determine the amount of H_2 adsorbed on a Pt catalyst supported on alumina previously reduced at 450 °C and the adsorption capacity evaluated at 25 °C [6]. The pressure range for the adjustment is between 100 and 300 torr. It has also been proposed to subtract the (reversible) physisorption isotherm from the combined isotherm as described above, and then extend a line tangential to the plateau of that isotherm to the zero pressure axis. Both methods should give approximately the same results, as long as the same analysis conditions are maintained. This value gives the amount adsorbed by weight of adsorbate. In the case of NH_3 adsorption, the ASTM D 4824–93 method proposes the adsorbed volume as that obtained at a pressure of 150 torr and a temperature of 175 °C [17] to minimize physisorption of ammonia. Additionally, repeated measurements at various temperatures can be used to calculate heats of adsorption (see next sections for details).

3.2. Isothermal dynamic volumetric procedure

In the case of the previous procedure, the surface of the solid to be analyzed must initially be free from any type of substance, that is, an initial heat treatment must be applied to clean the surface. Next, consecutive small amounts of adsorbate are added to allow the adsorption isotherm to be built, which means that a system that allows for the dosed volumes to be measured, as function of the increasing pressure. All this is performed under equilibrium conditions. Another possible procedure involves the solid sample being subjected to a stream of an inert gas to clean the surface and, subsequently, a known volume of the adsorbate gas being injected into this inert stream. This procedure has the following advantages: the measurements are fast compared to volumetric measurements; the weak bonds between adsorbent and adsorbate are not detected; the dead-volume need not to be measured; and the measurement can be easily tuned for small amount of samples.

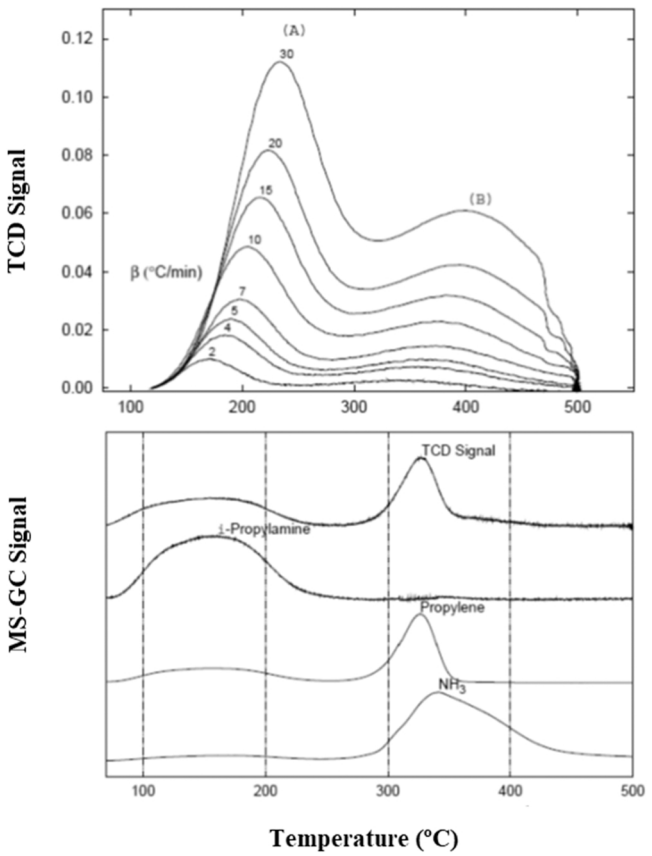

Fig. 4. TPD curves for ammonia, including the effect of heating ramp on the curve shape, and isopropyl amine, including compounds detected by GC-MS.

Thus, the adsorption centers can retain the adsorbate gas until the surface is completely covered, that is, until it is saturated (see Fig. 3) [18]. If the adsorption isotherm is previously constructed, then, and, after calibration of the signal, the amount adsorbed will be obtained (V_m, see Eq. 1). This case requires a system for detecting adsorbate gas in a gas stream, which is normally achieved by using a thermal conductivity detector (TCD).

$$V_m = \frac{\sum_{i=1}^{i=n}\left(h_{saturation} - h_{injected}\right)}{h_{saturation}} \cdot V_{injected} \quad (1)$$

where V_m is the volume of the chemisorbed monolayer, expressed in cm^3 at standard temperature and pressure (STP), $V_{injected}$ corresponds to the loop volume previously calibrated and its volume is continuously monitored by the system for any temperature and pressure change in order to deliver a corrected number of moles at each injection, $h_{injected}$ is the peak area corresponding to the injected volume. $h_{saturation}$ corresponds to the injected volume that produce same peak area, and indicate saturation or end of the analysis is reached. Some practical advice can be suggested for this method: the relation between the amount of adsorbate gas injected and the sample mass should be adjusted to ensure at least one the injected dose to be completely adsorbed by the sample, the interval of time between the pulses should be constant and long enough to allow for the TCD signal to return to base line, and consecutive pulses should be injected until no increase of the signal area for consecutive pulses can be detected.

3.3. Temperature-programmed desorption

In the two previous procedures, the working temperature remains constant. However, there is the possibility of repeating the analyses under other temperature conditions, which may allow additional information regarding the heat of adsorption to be obtained, or a method that enables the temperature to be increased to obtain information about the strength of adsorption to be used. This would be the case for the temperature-programmed desorption (TPD) procedure. In this case, upon sample saturation with a specific adsorbate, desorption can be carried under a specific ramping rate. If this analysis is repeated and desorbed at a different ramping rate, say (3, 5, 10, 15 and 20 ℃/min), thus would yield information about the strength of the adsorption centers (Fig. 4). This is the case for the adsorption of bases such as NH_3 or other amine molecules, as well as CO_2 [10]. As a gas stream that is in continuous contact with the solid is required, the detector used could also be a TCD. If no re-adsorption of gas takes place during desorption, and provided the molecules are adsorbed on a homogeneous surface without mutual interactions, the maximum temperature peak (T_m) can be related to the activation energy of desorption (E_d), see **Equation 2** [19]:

$$2\ln T_m - \ln\beta = \frac{E_d}{R \cdot T_m} + \ln\left(\frac{E_d \cdot V_m}{R \cdot k_d}\right) \quad (2)$$

where β is the rate of linear temperature increase, V_m is the amount adsorbed at saturation, and k_d is the pre-exponential factor in the expression for the desorption rate. If the kinetics of desorption are first order, it is possible to calculate E_d. In the case of the presence of surface heterogeneities (large surface areas and microporosity), deviations could be found.

The acidic or basic nature of the centers cannot be determined by this method, although it is possible to calculate the change in desorption activation energy with surface coating. If it is not possible to measure the amount of base adsorbed, or the amount that remains after desorption, the method can only give qualitative or semi-quantitative information (which can be obtained from the TPD profile).

4. Quantitative analysis: how to characterize the surfaces of adsorbents and metal catalysts

As a chemical bond forms between the adsorbate molecule and a specific center on the material surface, the number of sites can be determined by measuring the amount of chemisorbed gas. Although this may appear to be an easy and simple process, it should be noted that, depending on the nature of the metals and gases concerned and the operating conditions (temperature, pressure, measurement method), chemisorption could be partially reversible. The terms reversibility and irreversibility only have an operational meaning and are more important in the case of dynamic methods. In metallic catalysts, the active center is often a metal atom, with examples of this including nickel and platinum for the hydrogenation of unsaturated carbon-carbon bonds [1]. However, several important metal oxides and other non-metal catalysts must also be considered. As an example, we can cite the case of iron, to which other promoters are added to favor the synthesis of ammonia. The metallic atoms are found forming islands or clusters, rather than being distributed individually, on an inert porous material that acts as a support and favors their dispersion and stability. In several cases, this situation is not clear. The size of these islands and clusters depends on the nature of the metal and the support, as well as the method used to deposit it (preparation method). In such a case, the exposed active centers can be determined by the gas adsorption method. For supported metal oxides, the same gases used in selective chemisorption on metals (H_2, CO, O_2 and N_2O) are not compatible, since they adsorb weakly on these surfaces: CO is only weakly adsorbed on metal oxides, and all exposed surface sites cannot be evaluated; H_2 adsorption involves reaction with the surface and subsurface lattice oxygen; and O_2/N_2O are not adsorbed on oxidized surfaces [8]. Adsorption of H_2 and O_2 at sub-ambient temperatures has been attempted to avoid the participation of subsurface lattice oxygen and lattice oxygen vacancies, respectively, but was unsuccessful in avoiding the participation of these

Table 1
Specific chemisorption information for adsorbates and metals [1].

Gas adsorbate	Advantages	Disadvantages	Metal	Suitable temperature (°C)
H_2	– Chemisorption simple – Physical adsorption negligible	– Possible formation of hydrides – Sensitive to impurities – Possible presence of residual hydrogen after reduction at high temperature	Pt Ni	0 – 35 -78, - 195
CO	Low dissolution	– Physical adsorption at low temperatures – Various forms of molecule link – Carbonyl formation – Sensitive to impurities	Pd, Pt Ni, Fe Co	25. - 35 -78, −195 -78, −195
O_2	Low adsorption on oxide support	– Physical adsorption at low temperatures – Bulk oxidation at high temperature	Pt, Ni Ag	35 200
Adsorption dissociative of N_2O			Cu, Ag	35

species [20]. However, small alcohols are adsorbed on dehydrated and/or evacuated oxides and allow the number of active surface sites to be quantitatively and selectively assessed. Thus, methanol is a highly reactive molecule that has been reported to be chemically adsorbed on oxides and allows quantitative determination of the number of surface active (Ns) centers. It has been observed that methanol follows several routes of chemisorption in oxides [21], depending on the nature of the metal oxide, and some of these reactions can occur and allow the quantification of adsorption centers:

$$CH_3OH + M - OH \rightarrow M - OCH_3 + H_2O$$

(M is a metal cation site)

$$CH_3OH + M - O - S \rightarrow M - OCH_3 + S - OH$$

(S is the oxide support cation site) by breaking open hetero-bonds

$$CH_3OH + [*] \rightarrow CH_3OH - [*]$$

([*] is a coordinatively unsaturated Lewis acid site).

It has been reported that the typical number of active surface sites on oxides is about 0.7×10^{15} sites/cm^2, which is about half the value for metals (1.2×10^{15} sites/cm^2), because the surface density of sites on oxides is less than on metals. The number of active surface sites on MoO_3, V_2O_5 and ZnO is significantly lower (0.1×10^{15}/cm^2) due to the presence of much less active exposed surface planes due to the presence of coordinatively saturated sites [22].

Stoichiometry: Knowing the relationship (*stoichiometry*) between an exposed metal atom and an adsorbate gas molecule is an important factor in this type of determination as many polyatomic gas molecules do not adsorb to a single active site. This is the case, for example, for the hydrogen molecule (H_2). It has been reported that hydrogen adsorbs dissociatively, that is, it separates into two atoms, each of which reacts with a single metal atom. Thus, a gas molecule has bound to two metal atoms (this is the case of Pt, Pd, Rh, Ru, Ir and Ni). As such, the stoichiometry is said to be two (2) for this surface reaction. Similarly, a molecule of adsorbate gas could associate with more than one metal atom without dissociating. This is the case for carbon monoxide (CO), which is normally expected to bind in a one-to-one ratio (Me-C═O) but could form a bridge between two metal atoms (Me-(CO)-Me). This situation would also result in a stoichiometry of two. Cases in which an excess of adsorption would result in a stoichiometry of less than one are not implausible. This is the case for the formation of hydrides (for hydrogen) and carbonyls (for carbon monoxide). These latter situations should be controlled and avoided in whatever way possible. In the case of O_2 the O-Metal stoichiometry is 1.0, although the possible formation of metal oxides and bulk metal oxides may modify this relation.

The value of the stoichiometric factor X_m can be determined, for example, by chemisorption measurements using metal powders with known specific surface areas. In general, the number of atoms per unit area for polycrystalline metal surfaces is not known. For hydrogen chemisorption up to full coverage, X_m, the average number of surface metal atoms associated with the adsorption of an adsorbed hydrogen molecule is assumed to be 2. However, some uncertainty also exists in this regard. Fundamental studies on hydrogen chemisorption on Ni yield solid evidence that strongly chemisorbed hydrogen atoms are attached to, or just below, so-called C_8 sites, which are the holes formed by a cluster of three densely packed Ni atoms above an octahedral interstice. The number of C_8 sites is equal to the number of Ni atoms in the (111) plane and thus, for the (111) plane of free metals, $X_m = 2$ is a realistic choice. The total adsorbate uptake, n_m, is also subject to uncertainties. In many group VIII metals (Ni, Pt, Pd, Ru, Rh), the H_2 chemisorption isotherm has the form shown in Fig. 2. The highest amount of hydrogen is adsorbed (strong chemisorption) at a pressure of less than 133.22 Pa (1 torr). Above that pressure, weakly chemisorbed hydrogen adsorption occurs, mostly of the order of 20–25 % of the strongly retained monolayer. The difficulty is that the transition pressure between strongly chemisorbed hydrogen and weakly chemisorbed hydrogen is not clearly defined. As such, the X_m value of 2 refers to strongly chemisorbed hydrogen only.

Several factors affect the accuracy of chemisorption methods. These include factors associated with the stoichiometric factor, the crystallographic heterogeneity of the surface, the presence of a support that theoretically does not chemisorb, the possible absorption or dissolution of the adsorbate gas in the metal, reconstruction of the surface atoms during the process of chemisorption, as well as contaminants adsorbed on the surface. The stoichiometric factor is usually not a problem when H_2 is used as the adsorbate, since it generally dissociates by adsorbing on catalytically important transition metals and chemisorbs with a stoichiometric factor of 2 (based on the H_2 molecule). For the other gases mentioned, obtaining an exact and constant stoichiometric factor may be difficult as adsorption of such molecules will highly depend on the surface of the adsorbent. Thus, for example, in the adsorption of CO on Pd/SiO_2, if analyzed by IR, two adsorption bands that correspond to the Pd-(CO)-Pd bridge and to the linear form Pd═C═O are observed. For particle sizes less than 10 nm, the geometry of the surface and, therefore, the stoichiometric factor depend on the size of the particle. Thus, in supported Pt catalysts, for small particles, the stoichiometric factor for CO adsorption can vary between 1 and 2. For metal particles larger than 10 nm, this effect disappears, and it can be considered constant.

From an experimental point of view, the amount of gas adsorbed is measured. Therefore, it is essential to establish the stoichiometry involved, knowing the nature of the adsorbate gas and the active site. This information can be obtained from the literature on catalysts or by direct measurement (see Table 1) [1].

Monolayer coverage: Once the amount of gas adsorbed by the sample (the adsorption isotherm) has been determined, the number of active centers can be calculated from the capacity of the monolayer, V_m. A number of graphical and numerical methods can be applied for that

purpose, and the most widely used are described below. In the case of the volumetric dynamic procedure, the adsorbed volume (V_m) would be obtained directly (see Eq. 1).

Extrapolation. This method involves plotting points on the adsorption isotherm until the plateau is reached (e.g, ASTM method D 3908–88 for H_2 adsorption on Pt/Al_2O_3 catalyst) [6]. In this region, the surface has become saturated with the adsorbate and monolayer formation has been ensured. If the pressure and the amount of gas dosed are increased, only additional physical adsorption occurs. The contribution of this physisorption can be explained by assuming that it is zero at zero pressure. If the line joining the points of the plateau is extrapolated to the value of zero pressure (intercept with the OY axis, the value of the monolayer is obtained. This value of V_m represents the total amount of chemisorbed gas irrespective of the exact nature of the bonding type (strong or weak; see Fig. 2).

Irreversible isotherm: Some applications require that only strong chemisorption centers be determined and physisorption or weaker chemisorption centers excluded. In these cases, it is necessary to obtain a second adsorption isotherm. After acquisition of the first isotherm, the sample is evacuated at the analysis temperature to desorb loosely bound gas molecules. Strongly adsorbed molecules remain bound to active centers on the sample surface. A second adsorption analysis is repeated to produce a second isotherm that would provide information on weak chemisorption and physisorption and is obtained in the same way as the first. The difference between the two isotherms at any given pressure represents the amount of chemisorbed gas. Alternatively, the plateau of the irreversible isotherm can be extrapolated to zero pressure to determine V_m graphically (see Fig. 2).

The above methods try to describe a simple (or pure) chemisorption process, although in some cases the interference of the catalytic support can be considered as it may have its own adsorption centers that can interfere with the process. This may be the case, for example, for the so-called *spillover* process in which the hydrogen that is dissociatively adsorbed on the metal (normally Pt) migrates to the surface and the bulk of the support. In cases where there is *spillover* (or at least there may be), two isotherms must be measured to determine the adsorption capacity: one for the supported metallic catalyst and the other for the support only (normally is known as blank), without the active metallic phase. The first isotherm yields adsorption data consisting of strong chemisorption at the active sites, weaker chemisorption, physisorption at the active sites and on the exposed support surface, plus active site *spillover*. The second isotherm simply consists of physisorption on the support. The net amount of chemisorption, including spillover, can be easily calculated by subtracting the second data set from the first.

4.1. Metallic surface

If the stoichiometric factor of chemisorption is known, it is possible to calculate the accessible number of surface atoms (N_S) of the component (generally metal) from the amount of adsorbed gas using Eq. 3:

$$N_s = \frac{V_m \cdot N_A \cdot X_m}{V_{mol}} \tag{3}$$

where V_m is the volume of the chemisorbed monolayer, expressed in cm^3 at standard temperature and pressure (STP); V_{mol} is the molar volume of adsorbate (22414 cm^3 occupied by one mol of gas at STP); N_A is Avogadro's number (6.022×10^{23}); and X_m is the average stoichiometric factor. X_m indicates the number of surface atoms of the component that are covered by an adsorbate molecule after chemisorption.

In many cases, the small metallic crystallites are firmly attached to the support via chemical bonds. As a result, the distribution of the crystallographic planes on the surface is, in most cases, different to the equilibrium distribution that would correspond to a free particle. Therefore, the value of N_S is strongly affected by support/particle interactions. The presence of the *SMSI* (strong metal/support interaction) effect can even completely suppress any form of hydrogen chemisorption. In this case, there would be no metallic species on the surface sensitive to chemisorption and therefore this cannot be evaluated.

Table 2
Useful physical parameters for metals commonly encountered during chemisorption studies.

Metal	Atomic mass	Density (g/cm^3)	Cross sectional area (nm^2/atom)
Chromium, Cr	51.996	7.20	0.0635
Cobalt, Co	51.933	8.90	0.0662
Copper, Cu	63.546	8.92	0.0680
Gold, Au	196.967	19.31	0.08696
Hafnium, Hf	178.490	13.10	0.0862
Iridium, Ir	192.220	22.42	0.0862
Iron, Fe	55.847	7.86	0.0614
Manganese, Mn	54.938	7.43	0.0714
Molybdenum, Mo	95.940	10.20	0.0730
Nickel, Ni	58.690	8.90	0.0649
Niobium, Nb	92.906	8.40	0.0806
Osmoum, Os	190.220	22.48	0.0629
Palladium, Pd	106.420	12.02	0.0787
Platinum, Pt	195.080	21.45	0.0800
Rhenium, Re	186.207	20.53	0.0649
Rhodium, Rh	102.906	12.40	0.0752
Ruthenium, Ru	101.070	12.30	0.0614
Silver, Ag	107.868	10.50	0.0870
Tantalum, Ta	180.947	16.65	0.0800
Thorium, Th	232.038	11.70	0.1350
Titanium, Ti	47.900	4.51	0.0741
Tungsten, W	183.850	19.32	0.0741
Vanadium, V	50.942	4.51	0.0680
Zirconium, Zr	91.220	6.50	0.0877

The specific metallic surface area, A_m, is determined as the product of the number of exposed metal atoms, N_S, by the cross-sectional area of each atom (see Table 2), A_X, and per unit mass, W (see Eq. 4):

$$A_m = \frac{N_s \cdot A_X}{W} \tag{4}$$

It can also be expressed per gram of metal in the catalyst if the experimentally determined metal content (%) is included (see Eq. 5).

$$A_m = \frac{N_s \cdot A_X}{W \cdot \frac{\%metal}{100}} \tag{5}$$

Another factor to consider when calculating the metallic surface (m^2 of metal/g) from chemisorption measurements is a lack of information about the heterogeneity of the crystallographic surface of the dispersed metal particles. In such a case, the number of accessible metal atoms on the surface can be calculated using Eq. 3. However, the calculation of the metallic surface requires information about the number of atoms per unit surface. This value is clearly defined in the ideal plane of a single crystal, but not for the case of metallic particles with surfaces exposing several crystallographic planes. To avoid this difficulty, the three most prominent planes—(111), (100) and (110) for cubic face-centered and (110), (100) and (211) for cubic body-centered—are generally considered to be present in equal numbers. As such, the number of atoms per m^2 of surface for face-centered metals (Ni, Pd) is $1.91 \times 10^{18}/\boldsymbol{a}^2$ and (Fe, W) is $1.35 \times 10^{18}/\boldsymbol{a}^2$ for body-centered metals, where $\boldsymbol{a}$ is the lattice constant. The specific metal surface of a supported metal catalyst can be calculated using Eqs. 4 or 5, where N_s is the number of accessible atoms on the metal surface per gram of catalyst.

4.2. Dispersion

In the case of supported metal catalysts, it is important to know what fraction of the active metal atoms is exposed and available to catalyze a reaction. This is a surface phenomenon as the atoms inside the metal particles do not participate in surface reactions. Hence, these atoms must be dispersed as widely as possible. Dispersion is defined as the

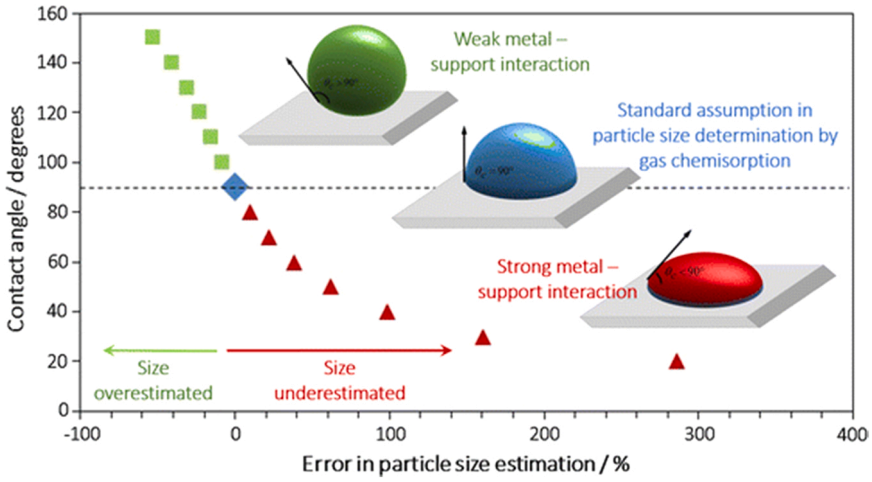

Fig. 5. Effect of the metal–support interaction on the shape of the metal particle and the error that is made in the measurement of the size [23].

percentage of all metal atoms in the sample that are exposed at the surface. As the total amount of metal in the sample can be determined by chemical analysis of the sample, if the weight of the metal in the catalyst is known, the degree of dispersion *D(%)*, that is, the ratio of atoms on the surface (N_S) with respect to the total number of atoms (N_T, atoms on the surface and in volume), of the metal can be calculated (see Eq. 6).

$$D(\%) = \frac{N_s}{N_T} = \boldsymbol{V_m} \cdot \frac{X_m \cdot M_{átomoMetal}}{V_{mol} \cdot \%_{metal}} 100 \tag{6}$$

Logically, if gas-adsorption techniques are used, the atoms on the surface will be those that can be evaluated by chemisorption, and it is precisely those atoms that can participate in gas-solid reactions. This property is important since it can affect both the selectivity and catalytic performance in supported metal catalysts.

4.3. Particle size

If both the mass of metal in the catalyst and its density are known, the volume of metal can be estimated. If the metallic surface area (A_m) is already known, the equivalent particle diameter, *d*, can be estimated by assuming a shape factor for the particle (see Eq. 7).

$$d = \frac{6}{A_m \cdot \rho_{metal}} \cdot \left(\%reduction \right) \tag{7}$$

This diameter is assumed to correspond to a hemisphere in contact with the surface of the catalytic support. The geometric factor (in this case 6) is identical if it is a totally spherical geometry. These two geometries have been reported as the most frequent for supported metal catalysts.

Metal–support interactions and metal particle shape play an important role in determining particle size by gas chemisorption. A hemispherical shape is usually assumed, but can give misleading results of up to one order of magnitude. In such a case, the metal particle sizes are underestimated when the metal strongly interacts with the support and overestimated when there is a weak metal–support interaction. The assumption of spherical shapes always underestimates the size of the particles, with this error being considerably smaller with regular geometries than that associated with the effect of the metal–support interaction due to its effect on the shape of the particle. Therefore, some authors have introduced a particle–support interaction factor when determining particle size by chemisorption.

As indicated in the Introduction, clusters and particles have unique chemical and physical properties that depend largely on their size. In the case of heterogeneous catalysis, a relationship between the size of the metal particle and its performance and selectivity for multiple systems is acknowledged, and the particle size can even determine whether or not a system is active.

High-resolution transmission electron microscopy (TEM) provides qualitative and semi-quantitative information on the size and shape distribution of metal particles, as well as their dispersion in the support. In this technique, the contrast depends on the ratio of the atomic numbers of the metal and the support, with small particles having a lower contrast than large ones. Particles with diameters smaller than 1–1.5 nm are considerably more difficult to detect, thereby limiting accurate quantification of the particle-size distribution. Although these instrumental limitations have been resolved in recent years to be able to quantify particle sizes on the sub-nanometric scale, this technique is still not commonly used because of its low availably. It is also possible to obtain information using X-ray diffraction (XRD), in this case regarding the crystal size from the broadening of the diffraction line. As in the case of electron microscopy, limitations appear for the smallest particles and for those that do not exhibit crystallinity. Gas chemisorption, typically using H_2 and CO as probe molecules, is widely used in combination with TEM and XRD to quantify the particle-size distribution, or alone to estimate the metallic surface area accessible to the molecule probe. As reported previously, this technique consists of measuring the number of probe molecules adsorbed on the metallic surface of a material. Knowledge of the stoichiometric factor for the number of adsorbed probe molecules per metal surface atom allows the metal surface area, mean particle size and metal dispersion to be calculated. It is widely accepted that one of the main limitations of gas chemisorption as a particle-size determination technique is the precise determination of the aforementioned stoichiometric factor, which largely depends on the arrangement of the surface atoms. Indeed, the probe molecule can form linear, double or triple adduct bridges, therefore its value ranges between 0.5 and 2 for a given metal. It has been reported that the effect of the interaction of the metal and a support (the contact angle between the two) on the determination of the resulting average particle size may be greater than the effect of the stoichiometric factor due to the conventional assumption of the hemispherical shape of the particle.

A well-accepted fact in the field of heterogeneous catalysis is that the method of metal deposition affects not only the resulting particle size and distribution, but also the metal–support interaction. For example, the deposition-precipitation method generally produces hemispherical metal particles in which the flat planes of the metal are attached to the support, while impregnation methods produce spherical particles with very weak interactions with the support. The type of metal–support interaction (strong or weak) can have a key effect on the catalytic behavior. It has also been possible to demonstrate, by means of high-angle annular dark field (HAADF) images taken in a STEM, that when interaction with the support is very strong, the morphology of the particles can be more similar to two-dimensional plates rather than three-

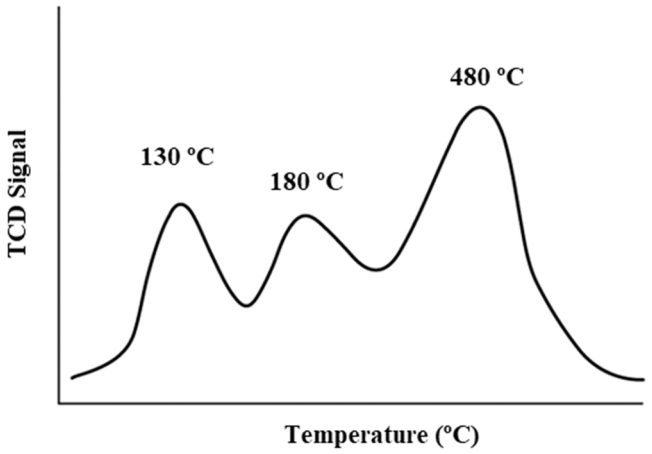

Fig. 6. TPD curves for hydrogen adsorbed on a Pt catalyst [11].

dimensional particles. Thus, the conventional assumption of metal particles with a hemispherical geometry for the calculation of average metal sizes by gas adsorption characterization can give misleading results if the metal particle is not hemispherical in shape. In fact, the metal–support interaction and, consequently, the resulting metal–support contact angle must be taken into account for an accurate estimate of the mean metal size. Particle sizes are slightly overestimated when their contact angle is $> 90^\circ$ (low interaction with the support); however, particle sizes are greatly underestimated when their contact angle is $< 90^\circ$ (high interaction with the support) (see Fig. 5) [23].

5. Active metals and gas adsorbates

When selecting the adsorbent gas to be used when using chemisorption measurements as part of the experimental method, it should be taken into account that the stoichiometric relationship that allows the quantity of metallic atoms on the surface to be determined should be known, thereby preventing the support from being able to adsorb or interact with the adsorbent gas [3,5]. Therefore, an initial study, including the operating conditions, is required for each metal to be analyzed to determine the most suitable conditions and adsorbents in order to determine the metallic atoms on the surface.

Pt catalysts: supported platinum catalysts, and how their dispersion is measured, are perhaps the most widely studied systems due to their widespread applications. The adsorption of hydrogen on Pt has been studied by several authors, who found that it is dissociative, that is, the H_2 molecule breaks and each atom binds to a different Pt atom. Adsorption is normally carried out at temperatures of between 0 and 35 °C. To try to clarify how H_2 is retained on the surface of Pt catalysts, these authors have conducted studies of hydrogen desorption at programmed temperature and found the presence of up to four states: **a)** hydrogen weakly adsorbed in a non-dissociative manner (–73 °C); **b)** hydrogen atoms adsorbed on the surface Pt atoms (130 °C); **c)** reversibly adsorbed hydrogen (180 °C); **d)** hydrogen *spillover* (480 °C; see Fig. 6) [11]. Of these states, it appears that option **b)** may have the highest possibility of being related to chemisorption. The possible contributions of the other states would cause errors in the determination of the amounts adsorbed. The stoichiometry accepted by most authors working with Pt catalysts is H_2:Pt = 1:2, although deviations from this stoichiometry may exist in the case of highly dispersed catalysts.

CO chemisorption has also been used in the characterization of Pt catalysts [24–26]. The main problems in this case are: **a)** the possibility of CO chemisorption in a linear (Pt-CO) or bridged (Pt-CO-Pt) form and, **b)** the possibility of formation of volatile carbonyls, and even other forms of triple bonds and dissociated molecules have been described [27–29]. The fact that one form or another predominates can cause the stoichiometry to be 1 or 2. The problem worsens because the relative proportion of these two forms depends on the particle size (the linear form predominates in high dispersions and the dotted form for particle sizes above 5 nm [30]). In general, it is considered that the two forms predominate, therefore a CO:Pt = 1:1.15 ratio is normally used. This situation is more common in the case of metallic catalysts containing Ni, Co, Ru, Mo, W, etc.

If the results obtained upon the adsorption of CO and H_2 on Pt are compared, the additional H_2 consumption observed can be explained by a *spillover* effect, which increases at high dispersions in which the metal–support interfaces increase. There may also be differences between the two measurements if the Pt is not fully reduced, in which case CO is adsorbed rather than H_2.

One alternative that has been proposed to increase the sensitivity to H_2 adsorption is H_2-O_2 titration reactions [31]. This method was proposed based on the chemisorption of H_2 and O_2 on Pt atoms on the surface, as well as on the reaction of H_2 with oxygen chemisorbed on Pt, and on the reaction of O_2 with hydrogen chemisorbed on Pt [32,33]. All these reactions are carried out at room temperature:

$$Pt + \frac{1}{2}H_2 \rightarrow Pt - H, \textit{hydrogen chemisorption } (HC)$$

$$Pt + \frac{1}{2}O_2 \rightarrow Pt - O, \textit{oxygen chemisorption } (OC)$$

$$Pt - O + \frac{3}{2}H_2 \rightarrow Pt - H + H_2O, \textit{hydrogen titration of oxygen covered surface } (HT)$$

$$2Pt - H + \frac{3}{2}O_2 \rightarrow 2Pt - O + H_2O, \textit{oxygen titration of hydrogen covered surface } (OT)$$

An HC:OC:HT:OT stoichiometry of 1:1:3:3 was initially proposed and the sensitivity of H_2-O_2 titration was found to be three times greater than for direct H_2 or O_2 chemisorption. More recently, some authors indicated that the results of the titration depend on pretreatment of the catalyst and on the titration procedure [34,35].

Pd catalysts: As in the case of Pt catalysts, CO adsorption can be used to characterize the metal surface of these catalysts [24–26]. The linear bond usually predominates, although it is necessary to control the conditions to ensure that this is the case [36–38]. Nevertheless, an average value of close to 2 was found for any support with dispersed Pd, although the measurements were performed using a pulse flow technique [39]. If hydrogen chemisorption is used to measure Pd dispersion, hydrogen absorption must be avoided. Thus, for example, exposure of supported Pd to a hydrogen atmosphere at room temperature results in the formation of β-Pd-Hx, where x decreases as Pd dispersion increases [40,41]. Starting from a 30 % dispersion, and heating above 70 °C, the absorption of hydrogen decreases considerably. Despite the absorption of hydrogen, the H:Pd ratio is considered to be 1:1 [42–45].

In catalysts of this family, the H_2/O_2 (or O_2/H_2) titration sequence has also been used as this technique has the main advantage that it allows the amount of adsorbed gas to be increased in catalysts with low dispersion. The reactions in this case would be [35]:

$$2Pd - H + 1.5O_2 \rightarrow 2Pd - O + H_2O$$

$$Pd - O + 1.5H_2 \rightarrow Pd - H + H_2O$$

Rh catalysts: in catalysts of this type, it has been reported that the CO:Rh stoichiometry can be 2:1, 1:1 and 1:2 [46], and even 1:3. In the case of supported Rh catalysts, 1:1 or 1:2 is proposed. If H_2 adsorption is used, it has been proposed that there is a 1:1 ratio, which is confirmed for low dispersions. The stoichiometry is 2:1 in the case of high dispersions [47–51].

Ni catalysts: the first drawback that can occur in this family of catalysts is that Ni is not completely reduced to the metal [52]. Although it can be assumed for the previous catalysts that all the metal is reduced, in the case of Ni catalysts this may not be the case [53]. A non-reduced

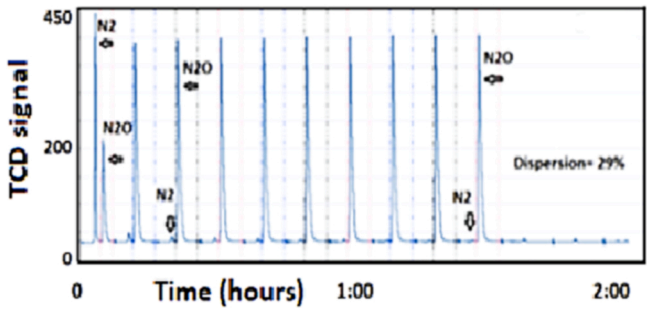

Fig. 7. Pulse chemisorption of N_2O on a 13 wt % reduced Cu/Al_2O_3 catalyst.

phase can be found between the support and the reduced metal particle, therefore this effect should be taken into account when calculating the metal dispersion [54]. In the case of some supports, such as alumina, this phase can be incorporated into the support by the formation of a spinel [55].

The formation of up to four $Ni(CO)_x$ complexes has been described, with the stoichiometry depending on the degree of dispersion and the adsorption temperature; therefore, the use of CO is not recommended when characterizing Ni catalysts [53]. The best method to characterize Ni-containing catalysts is the chemisorption of H_2 at temperatures of between 0 and 35 °C and at a pressure of up to 10–20 kPa. The stoichiometric factor in this case is 2 [53,56,57].

Cu catalysts: for this type of catalyst, H_2 chemisorption is not a good option due to its low sensitivity at low temperature. CO chemisorption cannot be used either, since it can be confused with physical adsorption. Alternatively, the adsorption of O_2 at −136 °C has been proposed. Under these conditions, the process is not activated and the stoichiometric factor is 4. However, the main drawback involves reaching the adsorption temperature. As an alternative, the adsorptive decomposition of N_2O at 90 °C is proposed:

$$N_2O(gas) + 2Cu \rightarrow Cu_2O + N_2(gas) + (\,Excess\ of\ N_2O\ that\ has\ to\ be\ trapped)$$

As the pressure remains constant during the process, nitrogen can be measured by assuming one N_2 molecule per two Cu atoms on the surface [58,59]. This method is also proposed for Ag and Ru. Although this method is rather difficult to be determined by the dynamic technique due to the fact that the TCD is not capable to differentiate between the peak of N_2 produced by the surface oxidation of Cu by N_2O and the excess of N_2O that does not react, Alternatively, a cold trap at − 80 ℃ is recommended to trap the excess of N_2O before reaching the TCD and allows the N_2 peak to pass on. Another useful alternative is to adapt a separation column that enables the separation of the N_2 peak from those corresponding to N_2O, thus the N_2 peak will arrive and be detected by the TCD before the delayed peak of N_2O reaches the TCD. In this case, the method becomes available to properly compute the amount of N_2 and to be related to the amount of Cu on the surface. This phenomenon of adversity can be easily resolved if a mass spectrometer is connected at the exhaust of the instrument. Example of this analysis is shown in Fig. 7.

Bimetallic catalysts: the presence of two metals makes it more complex to characterize the superficial metallic centers, specifically to know the stoichiometric relationship between the adsorbate gas and the metal. In these cases it is normally necessary to use other characterization techniques such as DRX or TEM. The simplest case for the use of chemisorption in bimetallic systems is when only one of the system components chemisorbs the adsorbate gas. For example, Ru-Cu and Os-Cu systems can be analyzed, since copper atoms do not adsorb hydrogen [60]. In Pt(Re,Ir,Ru) systems, selective chemisorption is performed by means of O_2/H_2 titration as it allows Pt and Re on the surface to be determined. The chemisorbed oxygen in Pt can be reduced by hydrogen at 25 °C, and a second titration with oxygen allows the Re atoms to be estimated by difference. This procedure can be used if the formation of alloys between metals does not occur. In the case of the Pt-Ru system, a titration using O_2 and CO is used following the same previous strategy [61].

6. Acidity/basicity by gas adsorption

In the case of acid centers, the nature of the surface must be taken into account, as well as the strength and number of centers [62]. First of all, it should be possible to differentiate between Brönsted- and Lewis-type acidity. In the former, a proton is brought into play as a Brönsted acid center is one capable of transferring a proton from the solid surface to an adsorbed molecule. This type of acidity can be generated when a trivalent ion is present in tetrahedral coordination with oxygen, with the most common example being aluminum [63]. When all the tetrahedral oxoanions are shared with two cations, a negative charge is created on cations with a charge of less than 4. This is the case, for example, in aluminosilicates [1]:

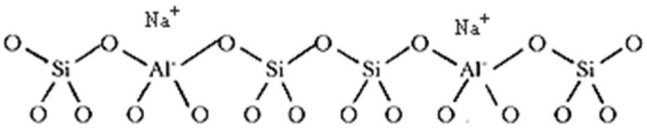

When the excess of negative charge is compensated with protons, silanol groups are formed, which can be presented as:

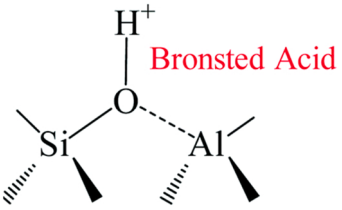

This is also a Brönsted center. In this case, the oxygen does not have a trigonal structure and is only represented as such to indicate that both Si and Al retain their tetrahedral coordination. This center is best detected by treatment with a basic molecule (e.g., an olefin) and subsequently observing the equilibrium:

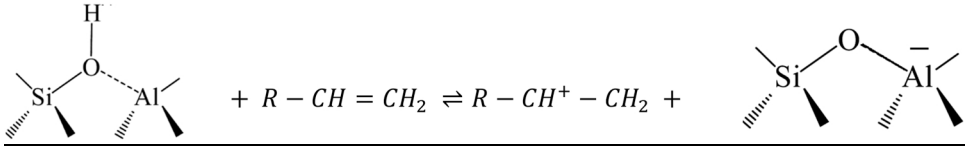

Depending on the strength of the Brönsted center, this balance can be displaced. The acidic surface is therefore dynamic and depends on both the chemical nature of the adsorbed base and the solid.

In Lewis-type acidity, the surface accepts an electron pair from the adsorbed molecule, forming a coordinate bond. In the case of silica-

alumina, this could be represented as [1]:

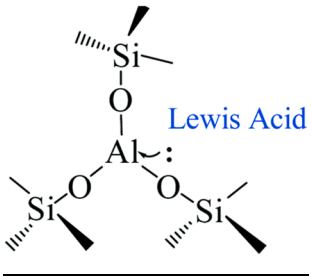

In the particular case of clays in which a dehydration point has not been reached and the exchange centers are occupied by cations such as Na^+, Ca^{2+}, Mg^{2+}, etc., the main Lewis centers are due to Fe(III) in the structure and the octahedral Al(IV) located on the edges of the particles [64]. Interactions between Brönsted and Lewis centers may also occur. Thus, for example, in a clay at 300 °C, the structural OH begins to be eliminated, forming trigonal Al(III) and H_2O. Dehydration processes accompany the formation of Lewis centers. Synergistic interactions between the Brönsted and Lewis centers may also occur. For example, an electron-deficient Al(III) (when in tetrahedral coordination) exerts an inducing effect on a neighboring silanol group, thus favoring H^+ mobility.

Depending on the nature of the surface, all materials, have an acid type and strength. The most representative acidic materials include alumina, silica-alumina, and zeolites, amongst others [65]. However, given the importance of this property, a series of solids known as superacids have been developed in recent years [66]. Treatment of activated carbons with acids (H_2SO_4, HNO_3) or other oxidants (H_2O_2, $Cr_3O_7^{2-}$, MnO_4^-) also creates acidic surface groups. Given the hydrophobic nature of the surface, these new centers will increase their hydrophilic character. The groups that have been proposed to exist on the surface of oxidized carbons are shown in Fig. 8 [67].

6.1. How to characterize the acidity/basicity of adsorbents

A solid of an acidic nature will not usually have a single class of acidity and will normally present a large distribution of acid centers. This may be due to a heterogeneity in the composition of the solid or the existence of a small range of interactions or surface structures. Both Brönsted and Lewis centers are often found in the solid at the same time. As such, it will be necessary to use methods that allows to differentiate and characterize a surface in terms of the nature, number, and strength of acid centers.

The titration of acid/basic centers using dynamic methods is carried out by injecting pulses of ammonia/carbon dioxide into a gas stream that allows the ammonia/carbon dioxide to pass through the adsorbent or catalyst bed at atmospheric pressure. This procedure has already been described above and allows the amount adsorbed, which is related to the capacity of the monolayer, to be determined. Similarly, it is possible to work in TPD mode. This method is the most commonly used in solid acid catalyst due to its simplicity and low cost and its ability to determine both the number of acid sites and their strength [68,69]. However, the use of ammonia presents limitations. Thus, ammonia is a small molecule that is able to penetrate the smallest pores of the material. However, these very small pores make a very small contribution to the catalytic behavior, therefore their contribution to the acidity of the material can be neglected. Additionally, it should be noted that ammonia is a base that can react with relatively weak acid centers and does not contribute decisively to the overall catalytic behavior. Typically, ammonia-TPD curves show two peaks (see Fig. 4), which may be related to the existence of at least two types of acid sites. The first peak (A) is related to desorption of weakly bound ammonia and was found to be of no catalytic relevance (it is relevant for gas-sensing applications); the other peak (B) reflects the desorption of ammonia probably from the Brönsted acid sites, which determines, for example, the acidic properties of zeolites. A classification related to weak, medium and strong acidic sites, related to the temperature of desorption peaks centered in the ranges 25–200, 200–400 and over 400 °C is also proposed [68], although there are currently no standardized criteria. Other larger molecules, such as pyridine or *tert*-butyl amine, isopropylamine, etc, are preferred because they only penetrate the largest pores and these are the ones that contribute most to the catalytic behavior observed. However, these molecules present operational problems since they can condense under operating conditions. The TPD of amines has recently been reported as technique for measuring Brönsted acid site concentrations. This method is based on the formation of alkylammonium ions from the adsorbed alkyl amines that are protonated by Brönsted sites, which decompose into ammonia and olefins in a range of temperatures. Typically, amine-TPD curves show two peaks (see also Fig. 4). The first peak is related to desorption of weakly bound amine and the other peak reflects the decomposition of amines at the Brönsted acid sites. In the case of isopropyl amine, propylene and ammonia would be obtained. The CO_2-TPD method allows analysis of the nature of basic sites. As in the case of ammonia, the strength of basic sites may be classified according to their different CO_2 desorption temperatures. In this case, the temperatures of desorption peaks below 400 °C, between 400 and 600 °C, and over 600 °C are related to weakly, medium and strongly basic sites.

Adsorption of the probe molecule and analysis by IR spectroscopy. There are numerous studies on the interaction of surfaces and basic molecules such as pyridine by IR spectroscopy [70,71]. Pyridine (C_5H_5N) is the preferred molecule to study Brönsted and Lewis acidity separately as these interactions can be easily distinguished from the IR spectra [72–74]:

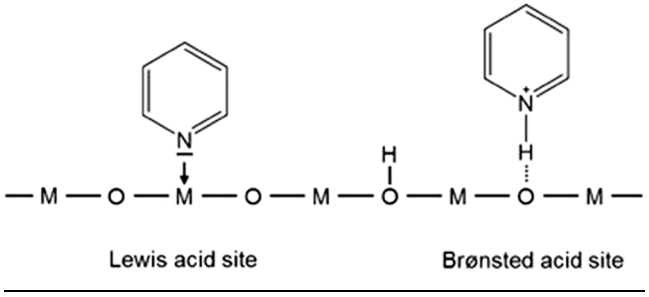

Other proposed molecular probes include acetonitrile (CH_3CN), benzonitrile (C_6H_5CN), CO, H_2 and NO. Direct measurement of the intensity of the frequencies of the OH groups does not provide information on the acid strength of the Brönsted centers and shifts in the frequencies of these vibrations by interaction via hydrogen bonds with adsorbed molecules provide more information. This interaction can be quantified as [75]:

$$\Delta\gamma = \frac{3qE}{4r(2\mu)^{1/2}D^{1/2}} \quad (8)$$

where $\Delta\gamma$ is the frequency shift of the hydroxyl group involved in the hydrogen bond interaction, q is the dipole charge, E is the electric field across the O-H axis, μ is the reduced mass, and D is the dissociation energy of the O-H bond. The values of $\Delta\gamma$ can be estimated, thus giving the Brönsted-type acid strength. The strength of the acid centers can also be studied from the evolution of these bands under different conditions of temperature and vacuum.

Pyridine is the most widely used molecule, since it is a weak Brönsted base ($pk_b = 9$) that only interacts with the strong protonic centers, that is, with the interesting ones from a catalytic point of view. The absorption bands of adsorbed pyridine are fine and allow Brönsted centers to be distinguished from Lewis centers. Information can be obtained on:

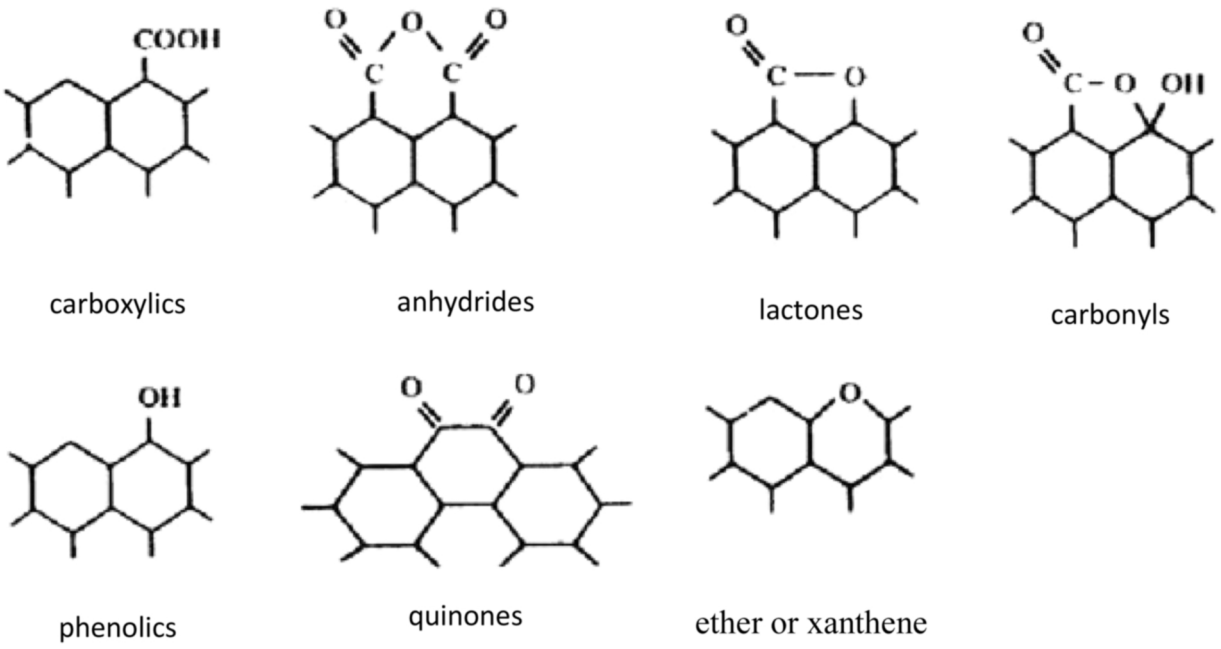

Fig. 8. Functional groups on the surface of activated carbons [67].

- The types of acid centers, as identified by the characteristic absorption frequencies.
- Their strength, from the variations in intensity of the bands upon desorption at increasing temperature.
- The reactivity of the OH groups with respect to the base, as seen from both the variation of intensities of the absorption maxima υ(OH) during adsorption and desorption, and by the positions of the reagent bands.
- The density of acid centers, from a plot of normalized absorbance (IR) against the amount of pyridine adsorbed.

In this case, information about the nature, density, and strength of the acid positions on the surface can be obtained. The nature of the interaction can be determined by assigning the frequencies of the physisorbed and chemisorbed pyridine bands in the 1400–1700 cm^{-1} region of the IR spectrum (see Table 3). The strength of these acid positions can be evaluated by exposing the sample to vacuum treatments and at several temperatures. The reference spectrum (baseline) corresponds to the sample prior to contact with pyridine. To evaluate the density of acid centers, a magnitude known as the normalized absorbance of the intensities must first be defined.

Table 3
Assignment of vibrational modes for pyridine (Py) adsorbed at Brönsted (B) and Lewis (L) acid sites.

Vibracional mode	PyF (cm^{-1})	PyL (cm^{-1})	PyB (cm^{-1})	PyH (cm^{-1})
8a	1580 – 1600 (s)	1615 – 1625 (s)	1638 – 1640	1595 – 1600 (s)
8b	1572	1575 – 1577 (v)	1620 (s)	1539 – 1575
19a	1485 – 1490 (w)	1485 – 1490 (v)	1485 – 1500 (vs)	1485 – 1490 (w)
19b	1439 – 1445 (vs)	1447 – 1460 (vs)	1540 – 1545 (s)	1447 – 1450 (vs)

(s): strong; (vs): very strong; (w): weak; (v): variable
PyF = physically adsorbed pyridine, bound by van der Waals-type interactions
PyL = pyridine adsorbed on nonprotic strong acid centers
PyB = pyridinium ions formed by protonation of pyridine and indicating Brönsted centers
PyH = pyridine H-bonded to surface OH groups

$$\frac{(absorbance)\cdot(n^{o}of\,wavelength)\cdot(mm^{2}IRbeamsection)}{(gof absorbent)}$$

Normalized absorbance represents an acid number that reflects the number of adsorbed species per unit area. It must be assumed that each acid center retains one adsorbed molecule. The sample is prepared in the form of a pellet, which is placed in a cell equipped with NaCl windows in which the sample can be degassed under vacuum and at a temperature of between 400 and 500 °C (depending on the previous treatment to which the catalyst has been subjected). After a desorption time, the sample is cooled to room temperature before being brought it into contact with pyridine for a short period of time. The sample is desorbed under vacuum at room temperature for 30 min to remove the physisorbed pyridine. Subsequently, it is subjected to vacuum and at several temperatures. At the end of each treatment, the IR spectra are recorded in the range 1300–4000 cm^{-1}. The spectra obtained upon subtracting the spectrum of the sample before pyridine adsorption and after each desorption are analyzed in the region from 3200 to 3700 cm^{-1} (O–H vibration) and in the region from 1400 to 1700 cm^{-1} (vibration of adsorbed pyridine). Various types of OH groups can be observed in the O–H vibration region (e.g., in PILC: structural hydroxyls and those related to pillared species) [64].

The frequencies assigned in Table 3 suggest that the adsorption bands located around 1620, 1575, 1490 and 1450 cm^{-1} are associated with coordinated pyridine (PyL), thus characterizing the Lewis-type acidity. In contrast, the bands at 1640, 1540 and 1490 cm^{-1} are due to the presence of pyridinium ions formed by the interaction with the protonic positions (Brönsted acidity). The band at 1545 cm^{-1} is most characteristic of the Brönsted-type acidity. The band around 1450–1455 cm^{-1} corresponds to a Lewis-type acidity if the sample has been previously degassed, since physisorbed pyridine exhibits a characteristic band at 1440–1445 cm^{-1}. The bands at around 1490 and 1620 cm^{-1} contain a contribution from both types of acidity. In addition, the band at 1620 cm^{-1} provides information on the strength of the Lewis-type positions: a shift towards higher frequencies (even above 1626 cm^{-1}) indicates the presence of a high Lewis-type acidity, whereas if the band moves towards lower frequencies (below 1615 cm^{-1}), the acidity of the centers is weaker.

It is also well known that CO can reach the Brönsted and Lewis acid

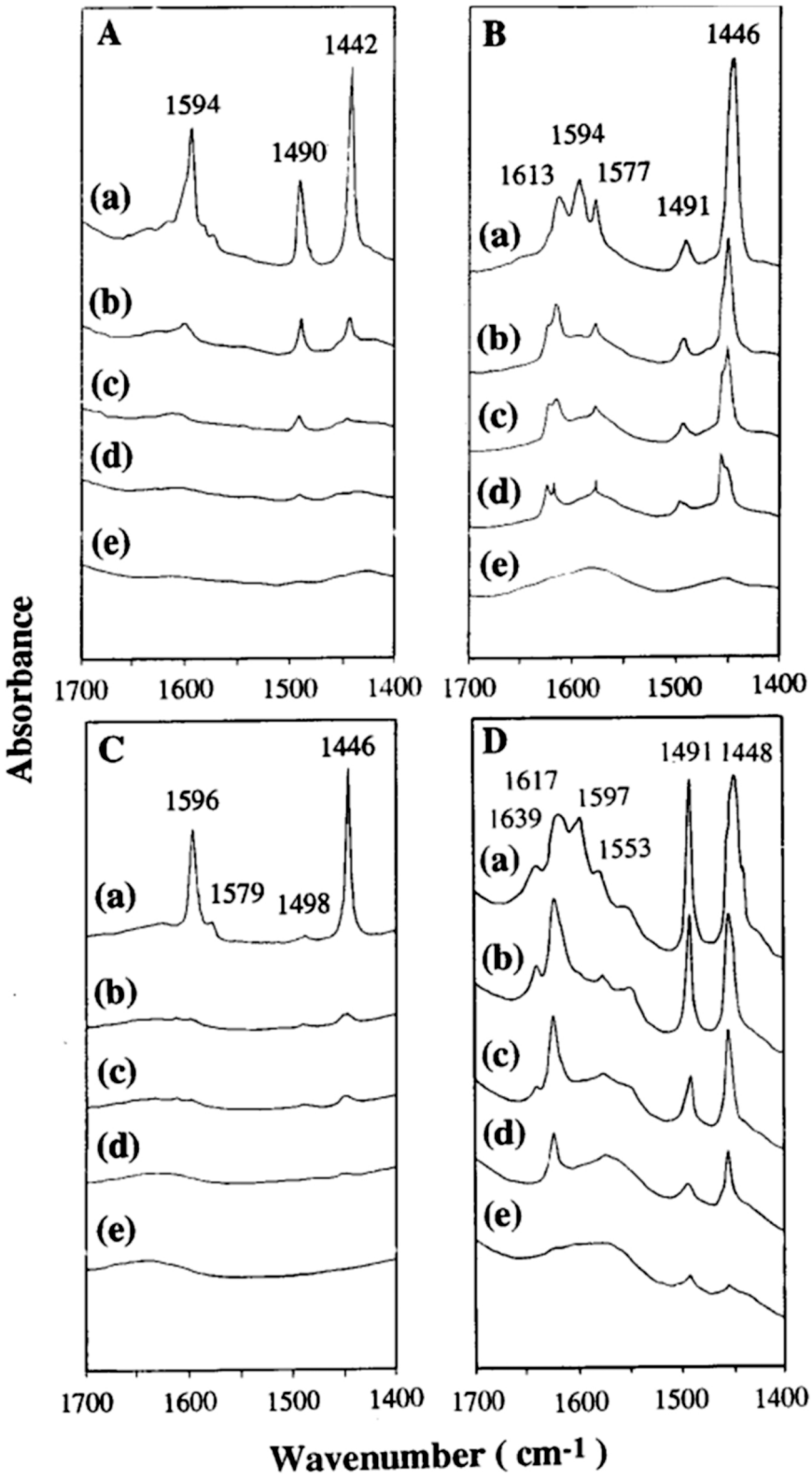

Fig. 9. FTIR spectra of pyridine adsorbed on montmorillonite (A), Al_2O_3 (B), SiO_2 (C), and Al-PILC (D). Sample spectra before pyridine adsorption (e); sample exposed to pyridine and outgassed at room temperature (a), 150 (b), 250 (c), and 400 °C (d) [73].

sites of microporous zeolites due to its small size [76,77]. This molecule allows determination of the oxidation state and environment of the metal cations on the surface and the amount and strength of Brönsted and Lewis acid sites.

Quantitative analysis: from the ratio of the absorbances of the bands due to pyridine adsorbed at a Lewis-type acid position and a band corresponding to pyridine adsorbed at a Brönsted position, the ratio of the Lewis and Brönsted-type acid positions multiplied by a constant K can be obtained ($\frac{L}{B} \cdot K$).

This expression comes from application of the integrated form of

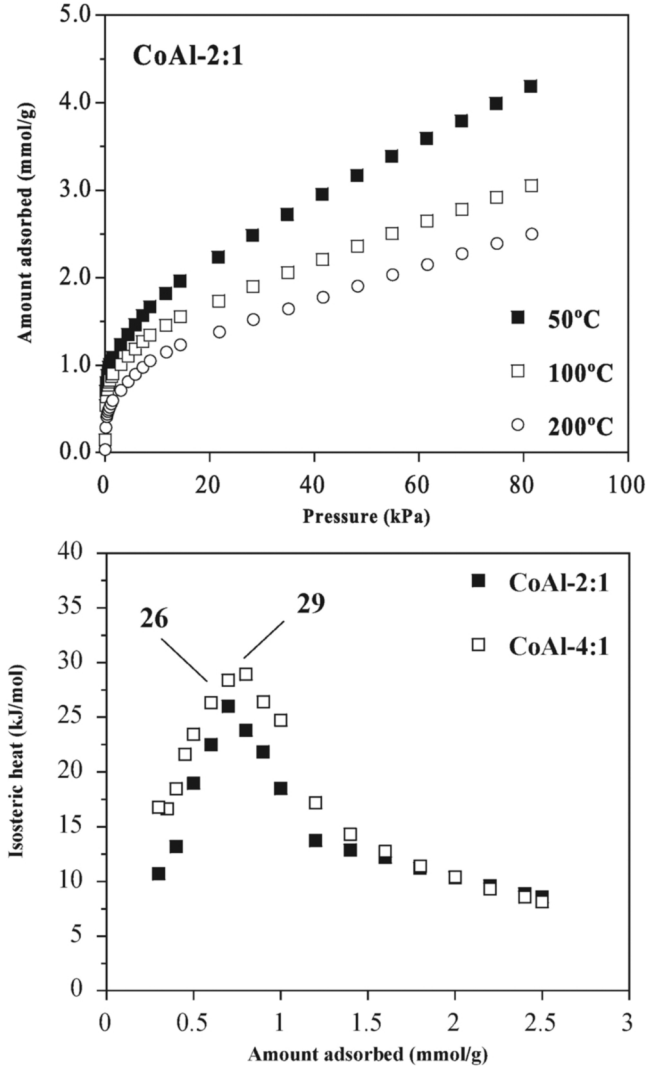

Fig. 10. CO_2 adsorption at various temperatures on a hydrotalcite CoAl and isosteric heat of CO_2 adsorption as a function of the amount of CO_2 adsorbed [90].

Beer's law [1]:

$$B = C{\cdot}L{\cdot}\int_{\gamma} \in_{\gamma}^{a}{\cdot}d\gamma \tag{9}$$

where B is the peak area (absorbance/cm), C is the concentration of the adsorbed species (mol/g), L is the tablet thickness (g/cm), $\boldsymbol{\gamma}$ is the wavenumber (cm^{-1}), and $\int_{\gamma} \in_{\gamma}^{a}{\cdot}d\gamma$, is the integrated apparent extinction coefficient (cm/mol).

The concentration of species at an IR absorbance maximum can be calculated assuming that the integrated apparent extinction coefficient is known. It can be determined if [1]:

$$\frac{\left(\int_{\gamma} \in_{\gamma}^{a}\right)_{L}}{\left(\int_{\gamma} \in_{\gamma}^{a}\right)_{B}} = \frac{2\left(B_{L}^{T_1} - B_{L}^{T_2}\right)}{B_{B}^{T_2} - B_{B}^{T_1}} \tag{10}$$

where the subscripts L and B refer to a specific IR band for pyridine (e.g., 1450 and 1550 cm^{-1}) and T_1 and T_2 to two treatment temperatures for the catalyst. The concentration relationship between the Lewis and Brönsted positions will be [1]:

$$\frac{[L]}{[B]} = \frac{B_L}{B_B}\frac{\left(\int_{\gamma} \in_{\gamma}^{a}\right)_{L}}{\left(\int_{\gamma} \in_{\gamma}^{a}\right)_{B}} \tag{11}$$

In the case described initially [1]:

$$\frac{[L]}{[B]} = \frac{L}{B}{\cdot}K, siL \equiv B_L yB \equiv B_B; K \equiv \frac{\left(\int_{\gamma} \in_{\gamma}^{a}\right)_{L}}{\left(\int_{\gamma} \in_{\gamma}^{a}\right)_{B}} \tag{12}$$

The best bands are 1450 cm^{-1} (19b vibrations of the coordinated pyridine) and 1344 cm^{-1}, although it must be considered the proximity of the band to 1447 cm^{-1} due to the presence of pyridine linked via a hydrogen bond that may affect the validity of the measurement. The band at 1610 cm^{-1}, which is also assigned to coordinated pyridine, can also be used, but in this case, there is likely to be a contribution of the band at 1639 cm^{-1} due to the pyridinium ion. Hence, in general, only the relationship between the sum of the Lewis positions (plus the protonic H positions due to the OH on the surface) and the Brönsted acid positions can be determined.

Other alternative methods, such as thermogravimetry and pyridine thermo-desorption, have been proposed to quantify the number of acid centers, depending on their strength. Thus, the evolution of the band at 1445 cm^{-1} can be evaluated as a function of the desorption temperature and quantified by representing the amount of pyridine adsorbed per mass of solid as a function of the absorbance per mass of solid.

Applications. A generic description of pyridine adsorption and its use in the characterization of acid centers in adsorbents and catalysts is difficult, so its study usually involves specific examples. Hence, herein it has been decided to use intercalated/pillared clays as study materials.

The acidity and nature of the acid centers (Brönsted and Lewis) depend on the cations exchanged, the method of preparation, and the nature of the clay [64,78–82]. In the case of aluminum-intercalated clays, Lewis-type acidity is related to two types of acid centers, both of which arise due to the aluminum present in the tetrahedral layer of the clay (LPy, 1641 cm^{-1}) and to the aluminum in the pillars (LPy, 1621 cm^{-1}) [83]. This latter center is the one that is usually related in the literature to Lewis acidity. In contrast, the origin of the Brönsted acid centers in the intercalated clays is not clear. These centers have been related to the structural hydroxyl groups of the clay layer, which in turn are related to the exchange centers, in other words, the protons of the oligomeric cations that form the pillars after heating, and to a synergistic phenomenon between the Si layer of the clay and the pillars [78,80–87].

When characterizing a hectorite intercalated with pillars of Al, ZrAl and Zr, Occelli observed that, after adsorption of pyridine and being subjected to vacuum (10^{-6} torr) at 300 °C, the natural hectorite presents both Brönsted and Lewis centers [84]. The pillars introduced affect the acidity observed in the initial clay. Thus, with only Al pillars, the characteristic PyH^+ bands (1638, 1547 and 1490 cm^{-1}) practically disappear or are significantly reduced in intensity, whereas with Zr and mixed ZrAl pillars, the pyridine is retained at both Brönsted and Lewis centers, even after degassing under vacuum and at 400 °C. At 300 °C and under vacuum in an intercalation with Al_2O_3, the pyridine is first removed from the Brönsted centers. In contrast, pyridine adsorbed at Lewis centers remains practically unchanged above 400 °C. The presence of Zr increases the Brönsted acidity in the intercalated hectorite. It is clear that the absolute intensities of the intercalated hectorite bands increase due to an increase in surface area.

In a study on montmorillonites intercalated with aluminum, the same author observed that, after being subjected to a vacuum at 400 °C, the pyridine continues to be found as PyH^+ and PyL. Proton acidity must be responsible for the instability of inorganic pillars at high temperature. Thus, when the pillars are formed by dehydration of the interlayer polymeric cation, protons are generated:

$$2\left[Al_{13}O_4(OH)_{24}(H_2O)_{12}\right]^{7+} \xrightarrow{\Delta} 13Al_2O_3 + 14H^+ + 41H_2O$$

At high temperature, these protons are able to react with the aluminum in the pillars in the same way that acids extract the aluminum from the zeolite structure.

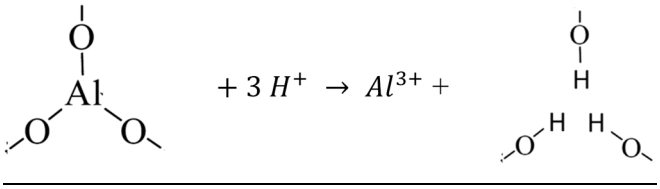

When this reaction occurs, the pillars decrease in size, and if Al^{3+} extraction continues, collapse occurs.

Fripiat et al. [88] reported that the most important acidity of the montmorillonite surface is due to hydrated H_2O molecules, which means that progressive dehydration can occur. Hence, comparing the pyridine and IR adsorption data obtained, these authors considered that both the Brönsted centers and the derivative of acid centers in intercalated montmorillonites decrease rapidly at 200 °C.

Despite the above, the actual nature of the acid centers in the pillars remains unknown. Assuming that the intercalated species is Al_{13}^{7+}, currently there are no information about the nature of its transformation after thermal activation at 300 °C, although the formation of a bayerite or gibbsite-type structure has been proposed [64]. In any case, protons from different sources must be the source of the acidity of pillared clays. These authors conclude by proposing that more than 90 % of the acid centers in both intercalated montmorillonites and calcined intercalated beidellites are of the Brönsted type, which are able to protonate pyridine to PyH^+ (band at 1640 cm^{-1}). Some examples of the adsorption and desorption spectra of pyridine adsorbed on different samples (montmorillonite, alumina, silica, and aluminum-intercalated montmorillonite) are shown in Fig. 9 [73].

Adsorption isotherm of the probe molecules. Acidic and basic centers can also be characterized using the static volumetric procedure described in Section 3.1. The amount of adsorbed gas (probe molecule) is obtained as a function of the equilibrium pressure at a constant adsorption temperature (see Fig. 10). The probe molecules used are those that characterize the acidic or basic properties of the adsorbent/catalyst listed above, such as CO_2, NH_3, pyridine (C_5H_5N), acetonitrile (CH_3CN), benzonitrile (C_6H_5CN), CO and NO, amongst others.

It is possible to quantify the adsorption capacity from the volume adsorbed at a given pressure and temperature. In the case of NH_3 adsorption, the ASTM D 4824–93 method proposes the adsorbed volume to be representative of that obtained at a pressure of 150 torr and at a temperature of 175 °C [17]. However, other parameters that allow the properties of adsorbents and catalysts to be characterized can also be calculated. Thus, Henry's constant is an important characteristic of adsorption because it provides an indication of the strength of adsorption and the isosteric heat of adsorption at low pressure. Although there are several possibilities for calculating Henry's constant [89], when it is obtained directly from the isotherm, this method is more accurate that others if sufficient data are available in the low pressure region.

The heat effects produced during adsorption processes can be described by the isosteric heat of adsorption and can be determined from the amount of gas adsorbed at several temperatures. The isosteric heat (q_{st}) defines the energy change resulting from the phase change of an infinitesimal number of molecules at constant pressure and temperature and a specific adsorbate loading. One method for calculating the isosteric heat of adsorption involves application of the Clausius–Clapeyron equation [89], which relates the isosteric heat to the pressure change of the bulk gas phase as a consequence of a temperature change for a constant amount adsorbed [89]:

$$q_{st} = -R \cdot \left[\frac{\partial \ln p}{\partial (1/T)}\right]_n \tag{13}$$

where p (kPa) is the equilibrium pressure, n is the amount of gas adsorbed at temperature T (K), and R (kJ/mol·K) is the universal gas constant. The isosteric heat can be obtained from the experimental isotherms at various temperatures by plotting $ln\ (p)$ versus $1/T$ for a constant loading n. The isosteric heat corresponds to the slope of the amount adsorbed by the materials, and the dependence of the isosteric heats of adsorption on the amount adsorbed can indicate the effect of surface loading. Indeed, in some cases, a maximum can be observed in the isosteric heats of adsorption in the presence of such a loading (see Fig. 10) [90]. This behavior can be related to the coating of the surface and subsequent formation of multilayers. Similarly, the limiting heat (q_{st}^0) can also be obtained from the temperature dependence of Henry's constant (H_i) by applying the Clausius–Clapeyron equation in the low-pressure region, where the isotherm obeys Henry's law.

$$q_{st}^0 = -R \cdot \left[\frac{d \ln H_i}{d(1/T)}\right]_{n=0} \tag{14}$$

The isosteric heats obtained from this last equation, and the values found from the isosteric heats at zero coverage, should be similar [90].

7. Summary and conclusions

The techniques and procedures presented in this work allow the characterization, evaluation, and determination of the qualitative and quantitative surface properties of adsorbents and supported metal catalysts by way of selective chemisorption processes.

The reaction behavior of a supported metal catalyst depends on the metal surface, the size of the metal particles, and how these particles are distributed on the surface of the catalyst support. Measurement of these properties using a chemisorption or selective adsorption technique requires careful selection of the operating conditions. Once established, however, chemisorption can be considered to be a method for routine measurement of the dispersion of supported metal catalysts. However, to measure the dispersion and particle size from the amount of an adsorbed gas, a series of assumptions are required, and it depends on the preparation and pretreatment conditions of the catalyst. A good practice, if possible, would be to use several adsorbates (H_2, CO, O_2), as well as to combine O_2/H_2 cycles and compare the results obtained. It will also be necessary to determine the possible effects of spillover, *SMSI*, presence of contaminants, and reversible adsorption. Among the techniques proposed, the isothermal dynamic procedure is the most popular since it allows faster measurements compared to the time needed to perform the volumetric measurements. In addition, in this case it is not necessary to volumetrically calibrate the equipment before or after the measurements. However, it has the drawback of only evaluating the centers where there is a strong interaction between the adsorbent gas molecule and the adsorption center.

Adsorbents and catalysts are characterized by having acid and basic centers that are involved in a large number of processes related to petroleum refining processes, amongst others. Two types of centers can be distinguished: Lewis and Brönsted. The most common technique to qualitatively characterize this type of center is to adsorb an acidic or basic gas molecule (NH_3 or CO_2) and perform its desorption in a programmed temperature ramp. However, the types of acid or basic adsorption centers cannot be differentiated using this procedure, therefore characterization is only qualitative. It is possible to characterize the desorption forces from the activation energy of desorption by modifying the heating rate. To be able to differentiate between adsorption centers, and even perform quantification, it is necessary to adsorb a molecule (pyridine, acetonitrile, benzonitrile, etc.) and conduct an analysis using IR spectroscopy. To characterize this type of center, it is increasingly common to use the static volumetric procedure, which allows the amount of adsorbed gas as a function of the equilibrium pressure at a constant adsorption temperature to be obtained. In addition to being able to quantify the adsorption capacity from the volume

adsorbed at a given pressure and temperature, it is possible to obtain Henry's constant and the isosteric heat of adsorption. The dependence of the isosteric heats of adsorption on the amount adsorbed can indicate the effects of surface loading.

CRediT authorship contribution statement

A.Gil: is the only author of this work. Conceptualization; Formal analysis; Investigation; Methodology; Resources; Supervision; Validation; Visualization; Writing - original draft; Writing - review & editing.

Declaration of Competing Interest

The authors declare that they have no known competing financial interests or personal relationships that could have appeared to influence the work reported in this paper.

Data availability

No data was used for the research described in the article.

Acknowledgements

The author express its gratitude to Dr Simón Yunes for valuable discussions and critical reading of the manuscript. The author is grateful for financial support from the Spanish Ministry of Science and Innovation (AEI/MINECO) and Government of Navarra through projects PID2020-112656RB-C21 and 0011-3673-2021-000004. Open access funding provided by Universidad Pública de Navarra. AG also thanks Santander Bank for funding via the Research Intensification Program.

References

[1] F. Delannay, Characterization of Heterogeneous Catalayst, Marcel Dekker, New York, 1984.
[2] J.R. Anderson, Structure of Metallic Catalysts, Academic Press, London, 1975.
[3] J.J.F. Scholten, A.P. Pijpers, A.M.L. Hustings, Surf ace characterization of supported and nonsupported hydrogenation catalysts, Catal. Rev. – Sci. Eng. 27 (1985) 151–206, https://doi.org/10.1080/01614948509342359.
[4] Z. Paál, P.G. Menon, Hydrogen Effects in Catalysis; Fundamentals and Practical Applications, Marcel Dekker, New York, 1987.
[5] J.A. Anderson, M. Fernandez-García, Supported Metals in Catalysis, in: Catalytic Science Series, Vol. 5, Imperial College Press, London, 2005.
[6] Standard test method for hydrogen chemisorption on supported platinum on alumina catalysts by volumetric vacuum method. D 3908–88. Annual Book of ASTM Standards, Section 5, Petroleum Products, Lubricants, and Fossil Fuels. 1999.
[7] A. Gil, M.A. Vicente, Energy storage materials from clay minerals and zeolite-like structures, in: M. Mercurio, B. Sarkar, A. Langella (Eds.), Modified Clay and Zeolite Nanocomposite Materials. Environmental and Pharmaceutical Applications, Elsevier, Amsterdan, 2019, pp. 275–288.
[8] D.A. King, D.P. Woodruff, The Chemical Physics od Solid Surfaces and Heterogeneous, in: Catalysis, Chemisorption Systems, Part A, Vol. 3, Elsevier Science Publishers, Amsterdam, 1990.
[9] J.C. Lavalley, Infrarred spectrometric studies of the surface basicity of metal oxides and zeolites using adsorbed probe molecules, Catal. Today 27 (1996) 377–401, https://doi.org/10.1016/0920-5861(95)00161-1.
[10] H. Hattori, Heterogeneous basic catalysis, Chem. Rev. 95 (1995) 537–558, https://doi.org/10.1021/cr00035a005.
[11] P.A. Webb, C. Orr, Analytical Methods in Fine Particle Technology, Micromeritics Instrument Corp. 1997.
[12] S. Lowell, J.E. Shields, M.A. Thomas, M. Thommes, Characterization of Porous Solids and Powders: Surface Area. Pore Size and Density, Kluwer Academic Publishers, 2004.
[13] S.J. Tauster, Strong Metal-Support Interactions, Acc. Chem. Res. 20 (1987) 388–394, https://doi.org/10.1021/ar00143a001.
[14] F. Rouquerol, J. Rouquerol, K. Sing, P. Llewellyn, G. Maurin, Adsorption by Powders and Porous Solids: Principles. Methodology and Applications, Elsevier, Amsterdam, 2014.
[15] R.I. Masel, Principles of Adsorption and Reaction on Solid Surfaces, John Wiley & Sons, Inc, New York, 1996.
[16] C. Hubert, A. Frennet, A new method for the determination of the monolayer capacity for hydrogen on a metal supported catalyst based on thermodynamic criteria applied to the, Catal. Today 17 (1993) 469–482, https://doi.org/10.1016/0920-5861(93)80050-B.
[17] Standard test method for determination of catalyst acidity by ammonia chemisorption. D 4824–93. Annual Book of ASTM Standards, Section 5, Petroleum Products, Lubricants, and Fossil Fuels. 1999.
[18] J. Friedland, B. Kreitz, H. Grimm, Th Turek, R. Güttel, Measuring adsorption capacity of supported catalysts with a novel quasi-continuous pulse chemisorption method, ChemCatChem 12 (2020) 1–15, https://doi.org/10.1002/cctc.202000278.
[19] R.J. Cvetanovic, Y. Amenomiya, A temperature programmed desorption technique for investigation of practical catalysts, Catal. Rev. – Sci. Eng. 6 (1972) 21–48, https://doi.org/10.1080/01614947208078690.
[20] B.M. Reddy, B. Manohar, E.P. Reddy, Oxygen chemisorption on titania-zirconia mixed oxide supported vanadium oxide catalysts, Langmuir 9 (1993) 1781–1785, https://doi.org/10.1021/la00031a028.
[21] G. Busca, Infrared studies of the reactive adsorption of organic molecules over metal oxides and of the mechanisms of their heterogeneously-catalyzed oxidation, Catal. Today 27 (1996) 457–496, https://doi.org/10.1016/0920-5861(95)00162-X.
[22] I.E. Wachs, Number of surface sites and turnover frequencies for oxide catalysts, J. Catal. 405 (2022) 462–472, https://doi.org/10.1016/j.jcat.2021.12.032.
[23] L. Torrente-Murciano, The importance of particle-support interaction on particle size determination by gas chemisorption, J. Nanopart. Res 18 (2016) 87, https://doi.org/10.1007/s11051-016-3385-2.
[24] A. Aznárez, F.C.C. Assis, A. Gil, S.A. Korili, Effect of the metal loading on the catalytic combustion of propene over palladium and platinum supported on alumina-pillared clays, Catal. Today 176 (2011) 328–330, https://doi.org/10.1016/j.cattod.2010.11.074.
[25] A. Aznárez, R. Delaigle, E. Eloy, E.M. Gaigneaux, S.A. Korili, A. Gil, Catalysts based on pillared clays for the oxidation of chlorobenzene, Catal. Today 246 (2015) 15–27, https://doi.org/10.1016/j.cattod.2014.07.024.
[26] A. Aznárez, A. Gil, S.A. Korili, Performance of palladium and platinum supported on alumina pillared clays in the catalytic combustion of propene, RSC Adv. 5 (2015) 82296–82309, https://doi.org/10.1039/C5RA15675K.
[27] P.J.A. Anderson, C.H. Rochester, Infrared study of CO adsorption on Pt–Rh/Al_2O_3 catalysts, J. Chem. Soc., Faraday Trans. 87 (1991) 1479–1483, https://doi.org/10.1039/FT9918701479.
[28] C. de la Cruz, N. Sheppard, An exploration of the surfaces of some Pt/SiO_2 catalysts using CO as an infrared spectroscopic probe, Spectrochim. Acta A Mol. Biomol. Spectrosc. 50 (1994) 271–285, https://doi.org/10.1016/0584-8539(94)80056-1.
[29] J.A. Anderson, CO oxidation over alumina supported platinum catalyst, Catal. Lett. 13 (1992) 363–369, https://doi.org/10.1007/BF00765039.
[30] T.A. Dorling, R.L. Moss, The structure and activity of supported metal catalysts: II. Crystallite size and CO chemisorption on platinum/silica catalysts, J. Catal. 7 (1967) 378–385, https://doi.org/10.1016/0021-9517(67)90166-2.
[31] J.E. Benson, M. Boudart, Hydrogen-oxygen titration method for the measurement of supported platinum surface areas, J. Catal. 4 (1965) 704–710, https://doi.org/10.1016/0021-9517(65)90271-X.
[32] D.E. Mears, R.C. Hansford, The stoichiometry for hydrogen titration of oxygen on supported platinum, J. Catal. 9 (1967) 125–134, https://doi.org/10.1016/0021-9517(67)90191-1.
[33] G.R. Wilson, W.K. Hall, Studies of the hydrogen held by solids. XIX. H_2 and O_2 chemisorption on silica-supported platinum, J. Catal. 24 (1972) 306–314, https://doi.org/10.1016/0021-9517(72)90074-7.
[34] D.J. O'Rear, D.G. Löffler, M. Boudart, Stoichiometry of the titration by dihydrogen of oxygen adsorbed on platinum, J. Catal. 121 (1990) 131–140, https://doi.org/10.1016/0021-9517(90)90223-7.
[35] G. Prelazzi, M. Cerboni, G. Leofanti, Comparison of H_2 adsorption, O_2 adsorption, H_2 titration, and O_2 titration on supported palladium catalysts, J. Catal. 181 (1999) 73–79, https://doi.org/10.1006/jcat.1998.2271.
[36] R. van Hardeveld, F. Hartog, The statistics of surface atoms and surface sites on metal crystals, Surf. Sci. 15 (1969) 189–230, https://doi.org/10.1016/0039-6028(69)90148-4.
[37] A. Palazov, G. Kadinov, Ch Bonez, D. Shopov, Infrared spectroscopic study of the interaction between carbon monoxide and hydrogen on supported palladium, J. Catal. 74 (1982) 44–54, https://doi.org/10.1016/0021-9517(82)90007-0.
[38] A. Corma, M.A. Martín, J. Perez-Pariente, A method for measuring the proportion of different plane orientations in metal supported catalysts by gas chemisorption, Surf. Sci. 136 (1984) L31–L34, https://doi.org/10.1016/0039-6028(84)90648-4.
[39] P. Canton, F. Menegazzo, S. Polizzi, F. Pinna, N. Pernicone, P. Riello, G. Fagherazzi, Structure and size of poly-domain Pd nanoparticles supported on Silica, Catal. Lett. 88 (2003) 141–146, https://doi.org/10.1023/A:1024001520260.
[40] G. Fagherazzi, A. Benedetti, S. Polizzi, A. di Mario, F. Pinna, M. Signoretto, N. Pernicone, Structural investigation on the stoichiometry of β-PdH_x in Pd/SiO_2 catalysts as a function of metal dispersion, Catal. Lett. 32 (1995) 293–303, https://doi.org/10.1007/BF00813223.
[41] M. Boudart, H.S. Hwang, Solubility of hydrogen in small particles of palladium, J. Catal. 39 (1975) 44–52, https://doi.org/10.1016/0021-9517(75)90280-8.
[42] J.P. Candy, V. Perrichon, Magnetic study of CO and C_2 hydrocarbons adsorption on $PdSiO_2$ catalyst, J. Catal. 89 (1984) 93–99, https://doi.org/10.1016/0021-9517(84)90283-5.
[43] M. Machida, D. Kurogi, T. Kijima, Role of hydrogen-spillover in H_2−NO reaction over Pd-supported NO_x-adsorbing material, MnO_x−CeO_2, J. Phys. Chem. B 107 (2003) 196–202, https://doi.org/10.1021/jp026321.
[44] M.A. Aramendia, V. Borau, C. Jiménez, J.M. Marinas, A. Moreno, Comparative measurements of the dispersion of Pd catalyst on SiO_2-$AlPO_4$ support using TEM and H_2 chemisorption, Colloids Surf. A Physicochem. Eng. Asp. 106 (1996) 161–165, https://doi.org/10.1016/0927-7757(95)03359-9.

[45] G. Prelazzi, M. Cerboni, G. Leofanti, Comparison of H_2 adsorption, O_2 adsorption, H_2 titration, and O_2 titration on supported palladium catalysts, J. Catal. 181 (1990) 73–79, https://doi.org/10.1006/jcat.1998.2271.

[46] R.R. Cavanagh, J.T. Yates Jr., Site distribution studies of Rh supported on Al_2O_3-An infrared study of chemisorbed CO, J. Chem. Phys. 74 (1981) 4150, https://doi.org/10.1063/1.441544.

[47] S.E. Wanke, N.A. Dougharty, Interaction of hydrogen, oxygen, and carbon monoxide with supported rhodium, J. Catal. 24 (1972) 367–384, https://doi.org/10.1016/0021-9517(72)90122-4.

[48] P.B. Rasband, W.C. Hecker, Catalyst characterization using quantitative FTIR: CO on supported Rh, J. Catal. 139 (1993) 551–560, https://doi.org/10.1006/jcat.1993.1048.

[49] J.C. Vis, H.F.J. van`t Blik, T. Huizinga, J. van Grondelle, R. Prins, The morphology of rhodium supported on TiO_2 and Al_2O_3 as studied by temperature-programmed reduction-oxidation and transmission electron microscopy, J. Catal. 95 (1985) 333–345, https://doi.org/10.1016/0021-9517(85)90111-3.

[50] H.C. Yao, S. Japar, M. Shelef, Surface interactions in the system $RhAl_2O_3$, J. Catal. 50 (1977) 407–418, https://doi.org/10.1016/0021-9517(77)90053-7.

[51] E.A. Hyde, R. Rudham, C.H. Rochester, Effects of preparation procedure on the surface properties of rhodium supported on γ-alumina, J. Chem. Soc., Faraday Trans. 1 (79) (1983) 2405–2423, https://doi.org/10.1039/F19837902405.

[52] A. Gil, A. Díaz, M. Montes, Passivation and reactivation of nickel catalysts, J. Chem. Soc., Faraday Trans. 87 (1991) 791–795, https://doi.org/10.1039/FT9918700791.

[53] C.H. Bartholomew, R.B. Panell, The stoichiometry of hydrogen and carbon monoxide chemisorption on alumina- and silica-supported nickel, J. Catal. 65 (1980) 390–401, https://doi.org/10.1016/0021-9517(80)90316-4.

[54] J.W.E. Coenen, Catalytic hydrogenation of fatty oils, Ind. Eng. Chem. Fundam. 25 (1986) 43–52, https://doi.org/10.1021/i100021a006.

[55] S. Narayanan, K. Uma, Studies of the effect of calcination on the dispersion and reduction of nickel supported on alumina by X-ray photoelectron spectroscopy, X-ray diffraction, chemisorption and catalytic activity, J. Chem. Soc., Faraday Trans. 1 (81) (1985) 2733–2744, https://doi.org/10.1039/F19858102733.

[56] J.A. Anderson, L. Daza, J.L.G. Fierro, M.T. Rodrigo, Influence of preparation method on the characteristics of nickel/sepiolite catalysts, J. Chem. Soc., Faraday Trans. 89 (1993) 3651–3657, https://doi.org/10.1039/FT9938903651.

[57] J.L. Carter, J.A. Cusumano, J.T. Sinfelt, Catalysis over supported metals. V. The effect of crystallite size on the catalytic activity of nickel, J. Phys. Chem. 70 (1966) 2257–2263, https://doi.org/10.1021/j100879a029.

[58] R.M. Dell, F.S. Stone, P.F. Tiley, The adsorption of oxygen and other gases on copper, Trans. Faraday Soc. 49 (1953) 195–201, https://doi.org/10.1039/TF9534900195.

[59] J.J.F. Scholten, J.A. Konvalinka, Reaction of nitrous oxide with copper surfaces. Application to the determination of free-copper surface areas, Trans. Faraday Soc. 65 (1969) 2465–2473, https://doi.org/10.1039/TF9696502465.

[60] J.H. Sinfelt, Supported "bimetallic cluster" catalysts, J. Catal. 29 (1973) 308–315, https://doi.org/10.1016/0021-9517(73)90234-0.

[61] H. Miura, R.D. Gonzalez, Methanation studies over well-characterized silica-supported Pt-Ru bimetallic clusters, J. Catal. 74 (1982) 216–224, https://doi.org/10.1016/0021-9517(82)90028-8.

[62] L. Forni, Comparison of the methods for the determination of surface acidity of solid catalysts, Catal. Rev. – Sci. Eng. 8 (1973) 65–115, https://doi.org/10.1080/01614947408071857.

[63] H. Knözinger, P. Ratnasamy, Catalytic aluminas: surface models and characterization of surface sites, Catal. Rev. – Sci. Eng. 17 (1978) 31–70, https://doi.org/10.1080/03602457808080878.

[64] J.-F. Lambert, G. Poncelet, Acidity in pillared clays: origin and catalytic manifestations, Top. Catal. 4 (1997) 43–56, https://doi.org/10.1023/A:1019175803068.

[65] R.T. Yang, Adsorbents: Fundamentals and Applications, John Wiley & Sons, Inc, Hoboken, New Jersey, 2003.

[66] K. Tanabe, H. Hattori, Solid Superacids, in: G. Ertl, H. Knözinger, J. Weitkamp (Eds.), Preparation of Solid Catalysts, Wiley-VCH Verlag GmbH, Weinhei, 1999, pp. 487–501.

67] R. Schlögl, Carbons, in: G. Ertl, H. Knözinger, J. Weitkamp (Eds.), Preparation of Solid Catalysts, Wiley-VCH Verlag GmbH, Weinhei, 1999, pp. 150–240.

[68] V.N. Panchenko, M.N. Timofeeva, S.H. Jhung, Acid-base properties and catalytic activity of metal-organic frameworks: A view from spectroscopic and semiempirical methods, Catal. Rev. – Sci. Eng. 58 (2016) 209–307, https://doi.org/10.1080/01614940.2016.1128193.

[69] R.J. Gorte, Temperature-programmed desorption for the characterization of oxide catalysts, Catal. Today 28 (1996) 405–414, https://doi.org/10.1016/S0920-5861(96)00249-0.

[70] C. Lamberti, A. Zecchina, E. Groppo, S. Bordiga, Probing the surfaces of heterogeneous catalysts by in situ IR spectroscopy, Chem. Soc. Rev. 39 (2010) 951–5001, https://doi.org/10.1039/C0CS00117A.

[71] J.A. Schwarz, B.G. Russell, H.F. Harnsberger, A study of pyridine adsorbed on silica-alumina catalysts by combined infrared spectroscopy and temperature-programmed desorption, J. Catal. 54 (1978) 303–317, https://doi.org/10.1016/0021-9517(78)90079-9.

[72] A. Gil, G. Guiu, P. Grange, M. Montes, Peparation and characterization of microporosity and acidity of silica - alumina pillared clays, J. Phys. Chem. 99 (1995) 301–312, https://doi.org/10.1021/j100001a046.

[73] A. Gil, M. Montes, Metathesis of propene on molybdenum-alumina-pillared montmorillonite, Ind. Eng. Chem. Res. 36 (1997) 1431–1443, https://doi.org/10.1021/ie960578a.

[74] E.P. Parry, An infrared study of pyridine adsorbed on acid sites. Characterization of surface acidity, J. Catal. 2 (1963) 371–379, https://doi.org/10.1016/0021-9517(63)90102-7.

[75] P.G. Rouxhet, R.E. Semples, Hydrogen bond strengths and acidities of hydroxyl groups on silica–alumina surfaces and in molecules in solution, J. Chem. Soc., Faraday Trans. 1 (70) (1974) 2021–2032, https://doi.org/10.1039/F19747002021.

[76] K.I. Hadjivanov, G.N. Vyassilov, Characterization of oxide surfaces and zeolites by carbon monoxide as an IR probe molecule, Adv. Catal. 47 (2002) 307–511, https://doi.org/10.1016/S0360-0564(02)47008-3.

[77] H. Knozinger, S. Huber, IR spectroscopy of small and weakly interacting molecular probes for acidic and basic zeolites, J. Chem. Soc. Faraday Trans. 94 (1998) 2047–2059, https://doi.org/10.1039/A802189I.

[78] F. Figueras, Pillared clays as catalysts, Catal. Rev. – Sci. Eng. 30 (1988) 457–499, https://doi.org/10.1080/01614948808080811.

[79] H. Auer, H. Hofmann, Pillared clays: characterization of acidity and catalytic properties and comparison with some zeolites, Appl. Catal. A: Gen. 97 (1993) 23–38, https://doi.org/10.1016/0926-860X(93)80064-W.

[80] S.M. Bradley, R.A. Kydd, Ga_{13}, Al_{13}, $GaAl_{12}$, and chromium-pillared montmorillonites: acidity and reactivity for cumene conversion, J. Catal. 141 (1993) 239–249, https://doi.org/10.1006/jcat.1993.1132.

[81] M.-Y. He, Z. Lin, E. Mim, Acidic and hydrocarbon catalytic properties of pillared clay, Catal. Today 2 (1988) 321–338, https://doi.org/10.1016/0920-5861(88)85013-2.

[82] D. Plee, F. Borg, L. Gatineau, J.J. Fripiat, High-resolution solid-state ^{27}Al and ^{29}Si nuclear magnetic resonance study of pillared clays, J. Am. Chem. Soc. 107 (1985) 2362–2369, https://doi.org/10.1021/ja00294a028.

[83] S. Bodoardo, F. Figueras, E. Garrone, IR study of Brönsted acidity of Al-pillared montmorillonite, J. Catal. 147 (1994) 223–230, https://doi.org/10.1006/jcat.1994.1133.

[84] M.L. Occelli, Physicochemical properties of pillared clays catalysts, in: S. Kaliaguine (Ed.), Keynotes in Energy-Related Catalysis, Stud. Surf. Sci. Catal, Vol. 35, Elsevier Science Publisher, Amsterdam, 1988, pp. 101–137.

[85] D.T.B. Tennakoon, W. jones, J.M. Thomas, Structural aspects of metal-oxide-pillared sheet silicates, J. Chem. Soc., Faraday Trans. 1 (82) (1986) 3081–3095, https://doi.org/10.1039/F19868203081.

[86] I. Khalfallah Boudali, A. Ghorbel, D. Tichit, B. Chiche, R. Dutartre, F. Figueras, Synthesis and characterization of titanium-pillared montmorillonites, Micro Mat. 2 (1994) 525–535, https://doi.org/10.1016/0927-6513(93)E0068-R.

[87] J.P. Chen, M.C. Hausladen, R.T. Yang, Delaminated Fe_2O_3-pillared clay: its preparation, characterization, and activities for selective catalytic reduction of NO by NH_3, J. Catal. 151 (1995) 135–146, https://doi.org/10.1006/jcat.1995.1016.

[88] J.J. Fripiat, J. Chaussidon, R. Touillaux, Study of dehydration of montmorillonite and vermiculite by infrared spectroscopy, J. Phys. Chem. 64 (1960) 1234–1241, https://doi.org/10.1021/j100838a028.

[89] S.I. Garcés-Polo, J. Villarroel-Rocha, K. Sapag, S.A. Korili, A. Gil, Comparative study of the adsorption equilibrium of CO_2 on microporous commercial materials at low pressures, Ind. Eng. Chem. Res. 52 (2013) 6785–6793, https://doi.org/10.1021/ie400380w.

[90] A. Gil, E. Arrieta, M.A. Vicente, S.A. Korili, Synthesis and CO_2 adsorption properties of hydrotalcite-like compounds prepared from aluminum saline slag wastes, Chem. Eng. J. 334 (2018) 1341–1350, https://doi.org/10.1016/j.cej.2017.11.100.